Cell-free Reconstitution of an Endoplasmic Reticulum-mediated Activation of MAPK/SAPK

by

Etienne Rousselle
Department of Anatomy and Cell Biology
McGill University
Montreal, Canada
August 2002

A thesis submitted to the Faculty of Graduate Studies and Research in partial fulfillment of the requirements of the degree of Master of Science

Your file Votre référence
ISBN: 0-612-88286-1
Our file Notre référence
ISBN: 0-612-88286-1

Table of Contents

Abstract

In response to stresses such as the accumulation of misfolded proteins, the Endoplasmic Reticulum (ER) triggers cytosolic and nuclear signalling events, which are integrated by the cell to result in adaptation or apoptosis. The activation of stress-responsive kinases (SAPKs) and the mitogen-activated kinases (MAPKs) are known to have a key influence cell fate determination. We developed a technique to study the regulation of these kinases by the ER in response to drugs inducing protein misfolding. We isolated ER-like compartments with a relatively high degree of purity using magnetic beads coated with anti-calnexin antibodies and we reconstituted in a cell free system the ER signalling induced by different stresses. We demonstrate here that ER-like compartments isolated from cells treated with azetidine-2 carboxylic acid or Tunicamycin differentially activates ERK-1, JNK-1 and p38 *in vitro*. Moreover, we show that the molecular adaptors Shc and Nck are involved in the ER-mediated regulation of these kinases.

Résumé

En réponse à divers stress comme l'accumulation de protéines mal repliées, le reticulum endoplasmique (RE) génère des événements signalétiques au niveau du cytoplasme et du noyau. De l'intégration de ces événements par la cellule résulte une adaptation au stress ou la mort par apoptose. L'activation des kinases sensibles au stress (SAPKs) et des kinases activées par les agents mitogènes (MAPKs) est reconnue pour avoir une influence clé sur la décision que prendra la cellule. Nous avons donc voulu étudier la modulation de ces kinases par le RE en réponse à diverses drogues provoquant le mauvais repliement des protéines. Pour ce faire, nous avons élaboré un système in vitro dépourvu de cellules où la modulation des kinases SAPK et MAPK est étudiées à l'aide de compartiments cellulaires s'apparentant au RE. Ces compartiments ont été isolés avec un degré de pureté relativement élevé en utilisant des billes magnétiques recouvertes d'un anticorps contre calnexin. Dans la présente étude, nous démontrons que ce compartiment active les kinases ERK-1, JNK-1 et p38 de différentes façons en fonction d'un traitement avec l'acide azetidine-2-carboxylique ou avec la Tunicamycine. Nous présentons également certaines évidences appuyant un rôle des adaptateurs moléculaires Shc et Nck dans la régulation de ces kinases effectuée par le RE.

Acknowledgments

I am sincerely grateful to my supervisor Dr. John J.M. Bergeron for his support and guidance. I owe him special thanks for giving me the chance of a second start in biological science research. He kindly accepted me in his lab after I experienced some difficulties in previous labs at the Montreal Neurological Institute where I first started my graduate work. During the last two years, I have been provided with an excellent research environment and skilful co-workers that allowed me to perform works on exciting topics. I also want to thank him for his enthusiasm, patience and encouragement regarding some side projects and hypothesis I had the chance to push forward.

I wish to thank Dr. Eric Chevet for all the work he has done in this project. Without his precious and outstanding collaboration, this study could never been presented here. I also want to thank him for the various lab techniques he taught me as well as for his patience and understanding. Through working at his side, I truly got the felling of what research is at superior degrees.

I would like to thank Dr. Louise Larose and Dr. Nathalie Lamarche for their helpful advice, encouragement as well as for the material and equipment they kindly provided during the last two years.

I also want to thank Ali Fazel for his precious collaboration and for all the skills and protocols he taught me. His patience and countless experience have been indispensable. Finally, I would like to thank Pam Cameron for her technical assistance and helpful advice.

Table of figures

List of abbreviations

ATP: Adenosine triphosphate
ATPase: Adenosine triphosphatase
AZC: Azetidine 2-carboxylic acid
bZip: basic leucine zipper
Ca++: Calcium ions
$[Ca^{2+}]_l$: Calcium concentration in the endoplasmic reticulum lumen
$[Ca^{2+}]_c$: Calcium concentration in the cytosol
CHOP: C/EBP homologous protein-10
CNX: Calnexin
CRT: Calreticulin
DTT: Dithiothreitol
EGF: Epidermal Growth Factor
EGFR: Epidermal Growth Factor Receptor
EOR: Endoplasmic reticulum overload response
ER: Endoplasmic reticulum
ERAD: ER-associated degradation
ERK1: Extracellular-regulated kinase 1
ERSE: ER stress response element (mammalian)
GADD: Growth arrest and DNA damage
GEF: Guanosine nucleotide exchange factor
GST: Glutathione s-transferase
GT: Glucose transferase
GTP: Guanosine triphosphe
GTPase: Guanosine triphosphatase
HRP: Horse Radish Peroxidase
Hsc70: Heat shock cognate 70
Hsp90: Heat shock protein 90
IRE1: Inositol requiring mutant 1
IP3R: Inositol (1,4,5)-triphosphate receptor
JIK: JNK inhibitory kinase
JNK: c-Jun N-terminal kinase
MAPK: Mitogen-activated protein kinase
MAPKK: Mitogen- activated protein kinase kinase
MAPKKK: Mitogen- activated protein kinase kinase kinase
MAPKKK: Mitogen- activated protein kinase kinase kinase kinase
MBP: Myelin basic protein
MEF:
NaAs: Sodium arsenite
NIK: Nck-interacting kinase
OST: Oligosaccharyltransferase
PAK: p21-activated Ser/Thr kinases
PBS: Phosphate buffer saline
PDI: Protein disulfide isomerase

PM: Plasma membrane
PMSF: Phenylmethylsolfoninyl fluoride
PP1: Protein phosphatase 1
PP2C: Protein phosphatase 2C
PS1: Presenilin-1
PTP: Phosphotyrosine-binding domain
PTP1B: Phosphotyrosine phosphatase 1B
Ptc2p: PP2C-like Ser/Thr protein phosphatase
QCM: Quality control machinery
RER: Rough endoplasmic reticulum
RM: Rough microsome
SM: Smooth microsome
ROI: Reactive oxygen intermediate
ROS: Reactive oxygen species
RTK: Receptor tyrosine kinase
S1P: Site 1 protease
S2P: Site 2 protease
SAPK: Stress-activated mitogen-activated protein kinase
SER: Smooth endoplasmic reticulum
SERCA: Sarco-endoplasmic reticulum Ca++-ATPase
SH2: Src homology-2
SRP: Signal recognition particle
TCA: Tri-carboxylic acid
SDS: Sodium dodecylsulfate
SR: Signal recognition particle receptor
TNFR: Tumor necrosis factor receptor
TRAF2: Tumor necrosis factor receptor-associated factor 2
Tun: Tunicamycin
Ubc: Ubiquitin-conjugating enzyme
UPR: Unfolded protein response
UPRE: Unfolded protein response element (yeast)
WGA: Wheat germ agglutinin
XBP-1: X-box binding protein 1

Literature review:

1-The endoplasmic reticulum of eukaryotic cells

The endoplasmic reticulum (ER) forms a convoluted network of interconnecting tubules and large cisternae enclosing a single internal space extending from the cell nucleus throughout the cytosol [1]. The ER membrane is continuous with the cell nucleus but not with the Golgi apparatus, which is the next organelle moving upward the secretory pathway. The ER is responsible for the synthesis of secreted proteins, lysosomal proteins and proteins that function in the organelles of the secretory pathway namely the ER, the Golgi apparatus and the plasma membrane. The ER is also involved in the first post-translational modifications of newly synthesized proteins, the Golgi apparatus being required for the further processing and the sorting of the proteins. The vehicles in which proteins are transported between the ER, the Golgi apparatus, and their final destination are known as coated vesicles. The portion of the ER termed rough ER (RER) is studded with ribosomes that are engaged in protein synthesis. The part of the ER devoid of ribosomes is named smooth ER (SER) and is involved in lipids synthesis [1]. Depending on the cell type, the SER may bear additional functions such as detoxification reactions in hepatocytes. The relative amount of SER and RER is influenced by the activities of the cells. Indeed, the pancreatic cells secreting a large amount of proteins for the digestion contain extensive regions of RER, which constitute 60 % of the total cellular membrane compared to 1% for the SER. In hepatocytes, the SER represent 16 % of the total membrane compared to 35% for the RER [2].

1.1-The ER lumen

The ER can maintain a high concentration of calcium ions, which makes it the main Ca++ cellular store. The Ca++ concentration in the ER lumen $[Ca^{2+}]_l$ undergoes continuous fluctuation since it is used as second messenger in cell signalling [3]. The steady state of $[Ca^{2+}]_l$ varies with cell types and it is usually three to four orders of magnitude higher than the Ca++ concentration found in the cytosol $[Ca^{2+}]_c$. [1,3] The ER lumen contains a high concentration of Ca++-binding proteins that help maintaining $[Ca^{2+}]_l$ homeostasis; some of them are chaperones involved in protein folding[3,4]. In fact,

the elevated $[Ca^{2+}]_l$ is thought to provide a favourable oxidative environment for the folding, the post-translational modification and the oligomerization of newly synthesized proteins. The Sarco-Endoplasmic Reticulum Ca++-ATPase (SERCA) family members are responsible for the ER uptake of Ca++ [5] .The ER Ca++ release is regulated through the Inositol (1,4,5)-triphosphate Receptor (IP3R) and the ryanodine receptor, which are Ca++ channels [5]. The regulated release of Ca++ from ER lumen is involved in many cellular signalling events related to cell mobility, cellular growth, apoptosis and the contraction of skeletal muscle fibres. Although the ER is an important cellular signalization target, it is also capable of sending stress signals to the nucleus upon disturbance of its protein processing functions [6]. For instance, disturbance of $[Ca^{2+}]_l$ that affect Ca++-binding chaperones leads to the accumulation of unfolded proteins and results in a ER-induced upregulation of genes encoding ER resident proteins involved in proteins folding.

1.2-Protein synthesis and modification

All secreted ER and lysosomal proteins, as well as many transmembrane proteins, are synthesized with an amino-terminal hydrophobic ER-targeting signal peptide (13 to 36 residues) [1]. This signal peptide, protruding beyond the ribosomal surface after the synthesis of the first 70 residues, is recognized by the signal recognition particle (SRP), leading to the arrests of the polypeptide elongation [7]. The SRP-ribosome complex is then targeted to the translocation machinery through the GTP-dependant interaction of SRP to the RER-localized transmembrane SRP receptor (SR). The translocation complex is mainly composed of the Sec61 complex (α,β and γ subunits) and TRAM as well as transiently associated proteins such as Bip [8]. Bip is an ER resident chaperone involved in protein folding; it as also been suggested to act as the molecular motor that powers polypeptide translocation [9]. The SR-mediated GTP hydrolysis leads to a succession of events including the release of SRP from SR and the ribosome and the binding of the ribosome to the translocon [8,10]. The protein synthesis also resumes after the departure of the SRP, and the elongation of the protein pushes the nascent chain through the translocon.

The folding and processing of the nascent proteins occurs both co-and post-translationally [11]. The signal peptidase proteolitically excise signal peptide when the nascent chain length totals ~150 residues[8]. Oligosaccharyltransferase (OST) glycosylates the nascent chain whenever an N-glycosylation sequence (Asn-X-Thr/Ser) extends more than 12-14 residues from the luminal end of the translocon. Protein disulfide isomerase (PDI) and ERp57, in complex with molecular chaperone such as calreticulin (CRT), calnexin (CNX), GRP94, and Bip, facilitates the correct disulfide bonds formation on newly synthesized proteins.

1.3-Quality control and ER exit

Misfolded and incompletely assembled proteins are common side products of protein synthesis in the ER. These proteins, under normal conditions, are recognized by the quality control machinery (QCM) and are not allowed to exit ER [12]. In fact, the QCM present within the ER ensures that only properly folded and assembled proteins that had correct co- and post-transcriptional processing are exiting the ER. The QCM works through multiple and partly overlapping mechanisms mainly carried out by the molecular chaperones mentioned above. When they recognize persistent misfolded or unassembled proteins they target them to the ER-associated degradation (ERAD) machinery [13].

QCM is particularly well characterized in the case of N-glycosylated proteins folding where it involves a mechanism known as the CNX cycle [14]. The basis of this mechanism rely on two homologous ER-resident lectins, CNX and CRT, which specifically associate with glycoproteins that have monoglucosylated trimming intermediates of their N-linked core glycans. Soon after its addition on newly synthesized proteins, the N-linked oligosaccharide gets two of its three glucose residues trimmed by glucosidases I and II, generating a monoglucosylated intermediate that binds to CNX/CRT [14]. The thiol oxidoreductase Erp57 then join the complex to form transient mixed disulfides bonds with the glycoprotein thereby promoting its folding. This complex dissociates upon the action of glucosidase II that cleaves off the remaining glucose. If the protein is still not correctly folded, it is recognized by the glucose transferase (GT) which reglucosylates the protein and the cycle is repeated [15]. A persistently unfolded glycoprotein gets marked for ERAD by the removal of one mannose

residue by mannosidase I. This intermediate is reglucosylation by GT but becomes a poor substrate for glucosidase II. The prolonged association with CNX/CRT triggers the retrotranslocation of the protein to the cytosol and its degradation by the proteasome [16]. A correctly folded protein get two mannose residues cleaved off by the mannosidase I and the mannosidase II, it is thus no longer recognized by GT and it is coupled to the cargo machinery to exit the ER [14,15].

Other mechanisms of quality control involve the formation of misfolded protein aggregates through the interaction with Bip, GRP94, CNX and CRT as well as with thiol oxidoreductases such as PDI and Erp72 [12]. Large protein aggregates cannot diffuse freely within the ER and are transport incompetent; they are also eventually targeted to ERAD. It should be noticed that transmembrane proteins synthesized in the ER contain folded domains on both side of the lipid bilayer. The folding occurring on the cytosolic side of the ER is assumed by cytosolic chaperones such as heat shock protein 90 (Hsp90) and heat shock cognate 70 (Hsc70), but whether or not these cytosolic chaperone associations can cause ER retention is not clear [12].

It is interesting to note that several diseases including Alzheimer disease and spongiform encephalopathies involve mutated proteins that cannot be recognized by the retrotranslocation machinery [17]. Their accumulation in the ER triggers an ER stress response leading to apoptosis and/or defects in differentiation. On the other hand, pathologies such as cystic fibrosis and hereditary emphysema originate from mutations in a particular protein and the further loss of coupling to ER export; the protein is thus degraded and can no longer achieve its function [17].

2-The unfolded protein response (UPR)

When cells are exposed to drugs triggering perturbations of protein folding and to various other environmental conditions such as glucose starvation, reducing conditions or viral infection, misfolded proteins accumulates in the ER [18]. The information that the folding capacity of the ER has been exceeded originates from the ER lumen and initiates the unfolded protein response (UPR), which transmits signals to the cytosol and the nucleus [19]. The UPR results in the up-regulation of genes encoding ER resident proteins and key enzymes of phospholipid biosynthesis as well as the suppression of protein

synthesis and increased ERAD activity. Some of the components of the UPR are conserved from yeast to mammals.

2.1-UPR in yeast

The UPR signalling cascade of the yeast has been the first well characterized and it revealed a completely unique pathway. The yeast UPR characterization began with the identification of a 22 bp cis-acting element of Kar2 (yeast homolog for Bip) gene promoter region sufficient to confer ER stress inducibility of a reporter gene [20]. This promoter region termed the unfolded protein response element (UPRE) allowed the cloning of the first member of the UPR signalling cascade, Hac1p, a basic leucine zipper (bZip) transcription factor [21]. An additional region upstream of Hac1p-binding site in the UPRE is also required for the full activation of the promoter. This region is thought to provide binding sites for constitutive transcription factors that collaborate with Hac1p. Since yeast strains lacking Gcn5p, Ada2p and Ada3p show partially defective for the UPR [21] and since cells lacking Ada5p are completely defective for the UPR [22], these transcriptional co-activators have been suggested to play a role in transcription from the UPRE.

Even though HAC1 mRNA is constitutively expressed, Hac1 protein is only synthesized after ER stress. This intriguing property is explained by the fact that activation of the UPR triggers the excision of a 252 nucleotides intron from the HAC1 mRNA, which prevented the translation of the protein [23]. Remarkably, this splicing event is not catalysed by the spliceosome but rather uses a unique splicing machinery composed of three proteins: the bifunctional Ire1p transmembrane kinase/endoribonuclease, Rlg1p, a tRNA ligase, and Ada5p, a transcriptional co-activator [24,25].

IRE1 was originally described as a gene required for inositol prototrophy (inositol requiring mutant) [18]. It encodes a type I ER resident transmembrane protein that contains both a Ser/Thr kinase domain and an endoribonuclease domain in its cytosolic portion; its luminal portion is suggested to act as a 'stress sensing' domain [26]. Ire1p was shown to be essential for cell viability during ER stress, being required for Kar2 and other chaperone upregulation during the UPR [24]. Both kinase inactive mutant and C-terminal endoribonuclease lacking mutant were shown to impair the UPR: endoribonuclease

activity of Ire1p is responsible for the HAC1 mRNA cleavage and the Ire1p kinase domain is essential for its activation by trans-autophosphorylation [26]. Recently, a direct role for Kar2p/Bip in the regulation of Ire1p was demonstrated [27]. Under unstressed conditions, Kar2p associates with the luminal domain of Ire1p preventing its trans-activation. Following ER stress, unfolded proteins accumulated in the ER segregate the chaperone from Ire1p, resulting in the trans-activation of Ire1p and the subsequent transmission of the UPR signal to the nucleus.

As explained above, HAC1 mRNA splicing is independent of the spliceosome machinery. It thus requires a special ligase to catalyze the religation of both ends of the HAC1 mRNA after Ire1p cleavage. The screen for yeast strains where UPR resulted in an Ire1p-dependant degradation of HAC1 mRNA, allowed the cloning of the RLG1 gene, which encodes the tRNA ligase responsible for HAC1 mRNA religation [28]. The HAC1 mRNA splicing may require other factors as suggested by Welihinda and coworkers who presented evidences for a role of the Ada5p transcriptional co-activator in the in vivo HAC1 mRNA cleavage mediated by Ire1p [25]. The same group also found the Ser/Thr phosphatase responsible for the downregulation of the UPR pathway [29]. They identified a novel PP2C-like Ser/Thr protein phosphatase termed Ptc2p that specifically interacts with phosphorylated Ire1p. Ptc2p was shown to dephosphorylate Ire1p in vitro, and yeast strains devoid of Ptc2p showed hyperactive Ire1p leading to deregulation of the UPR.

2.2-Mammalian UPR

The mammalian UPR shares some similarities to the yeast UPR but it is more diverged in both the key players in the pathway and its output [23]. Indeed, the metazoan UPR seems to involve at least four distinct ER stress signalling molecules: Ire1α, Ire1β, PERK and ATF6.

2.2-A-Ire1

Two different mammalian homologues for the yeast Ire1p have been identified in human: Ire1α and Ire1β [30,31]. While the Ire1 beta isoform expression is largely limited to the gut epithelium, the alpha isoform is ubiquitously expressed [24,30]. Both proteins show a high degree of homology to each other and to the yeast Ire1p kinase. For instance, exogenously expressed Ire1 can cleave yeast HAC1 mRNA in vitro, and the yeast UPR

signalling is preserved when the Ire1α luminal domain replaces the one in Ire1p [30,32]. The mechanism of activation of Ire1s, which involves Bip, and the signalling effects are also conserved in mammalians [33,23]. However, the importance of Ire1s in the mammalian UPR is still a matter of debate since MEFs isolated from both IRE1α -/- and IRE1α-/-:IRE1β-/- mice displayed a normal ER stress response [23,24]. Nevertheless, Ire1α is essential for mouse embryonic development.

Whether or not the mammalian Ire1 proteins exert their downstream effects on gene regulation by splicing a substrate mRNA was unknown until the recent discovery that XBP-1 mRNA undergoes an Ire1-dependant HAC1-like splicing during UPR [34]. XBP-1 was first identified as a transcription factor binding to the *cis*-acting X box (X-box binding protein) present in the promoter regions of human major histocompatibility complex class II genes [35]. Mori's group rediscovered XBP-1 in a yeast screen using the mammalian ER response element (ERSE), which is a cis-acting element necessary and sufficient for the induction of the mammalian UPR [36]. XBP-1 is similar to yeast HAC1 only in that both proteins are bZip transcription factors. Even if the splicing mechanism is conserved, many of its features have diverged [34]. Unlike HAC1 mRNA, the Ire1-excised XBP-1 fragment consists only in 26 nucleotides, which is too short to form a translation inhibitory structure. Instead of relieving a translation repression sequence, this deletion induces a frame-shift in the C-terminal portion of XBP-1; the resulting protein has the original N-terminal DNA binding domain, but a new C-terminal transactivation domain. The XBP-1 mRNA is expressed at a low level in unstressed cell and it is constitutively translated. Importantly, this mRNA must be induced to a significant level to produce the spliced form of XBP-1 at the quantity sufficient for detection and transactivation of ERSE [34]. The induction of XBP-1 mRNA appears to be regulated by another transcription factor, ATF6, which may have a more important function than XBP-1 in the mammalian UPR [34]. Finally, some reports suggested that Ire1a mRNA [37] and 28S ribosomal RNA [38] might also be targets of Ire1's endoribonuclease activity. However, the role these effects might play in inducing downstream components of the UPR remains elusive.

2.2-B-ATF6

Although ERSE contains binding site for the general transcription factors CBF/NF-Y, YY1 and TFII-I, it is specifically activated upon binding of the ubiquitous bZip transcription factor ATF6 [39-41]. Like HAC1, ATF6 is a member of the ATF/CREB protein family, but instead of being regulated by splicing it is regulated by proteolytic cleavage. ATF6 protein is constitutively expressed as an ER-localized type II transmembrane glycoprotein with a luminal stress sensing domain and a cytosolic transcription transactivation domain [39]. Upon ER stress, the transactivation domain of ATF6 is cleaved by sequential action of site 1 protease (S1P) and site 2 protease (S2P). Intriguingly, these two proteases are localized to the Golgi apparatus; ATF6 must therefore be translocated to this organelle to be cleaved [42]. Even though the luminal portion of protein is required for the proteolytic activation of ATF6, the exact mechanism by which this transcription factor is activated upon ER stress remains unclear. The role of ATF6 during the mammalian UPR is thought to be more important than Ire(s) since cells lacking Ire1a have no obvious defect in Bip induction [20]. Indeed, dominant negative ATF6 constructs strongly inhibited the induction of UPR target genes in vivo, and cells that lack S2P (being unable to cleave ATF6) are largely deficient in ER-stress induced Bip expression [43]. Recently, Mori's group identified another bZip transcription factor closely related to ATF6 encoded by the gene G13; this protein was termed ATF6β while ATF6 was renamed ATF6α [44]. ATF6β is an ER-localized type II transmembrane glycoprotein that is proteolitically activated during UPR and the cleaved transcription factor binds to the ERSE. The formation of ATF6α/ATF6β heterodimers has been suggested to be involved in the regulation of the activation of ERSE.

Regulated proteolysis may play another role in the UPR since Ire1a and Ire1b have been shown by two groups to translocate in a soluble form to the nucleus [45,46]. The redistribution of Ire1 to the nucleus would require proteolytic cleavage by presenilin-1 (PS1), a protein associated with the activity of γ-secretase in the proteolytic regulation of the transcription factor Notch during the development. However, the largest observed effect of PS1 gene disruption on Bip induction is less than three-fold, and a third group observed no effect of PS1 expression on induction of UPR target genes [47]. Thus, the role of PS1 in UPR activation remains controversial.

2.2-C-PERK

Mammalian UPR involves a third ER-localized ER stress-induced kinase termed PERK. PERK is transmembrane protein presenting the ER-luminal features of Ire1p but containing Ser/Thr kinase domain related to the eIF2α kinase family in its cytosolic portion [48]. Similarly to what is observed for Ire1p, the accumulation of unfolded proteins during ER stress triggers the dissociation of Bip from PERK, which allows PERK to oligomerize and *trans*-autophosphorylate [33]. Like other members of the eIF2α family of kinases activated in response cellular stresses, PERK down-regulates the overall protein synthesis by phosphorylating eIF2α, which inhibits of the assembly of the 80S ribosomal initiation complex [49,50]. The subsequent translational slowdown protects cells from the toxic effects of unfolded protein accumulation by preventing additional synthesis of proteins under conditions that do not allow proper folding. Profound alterations of the UPR are observed in mice bearing a homozygous eIF2α mutant (S51A) that can no longer be phosphorylated by PERK, and PERK knockout cells are particularly sensitive to ER-stress-induced apoptosis [51,52]. Through the translational downregulation of cyclin D1, which is a protein required for S phase transition, PERK also promotes a growth arrest in the G1 phase [53]. Concomitantly, cells overexpressing cyclinD1 were also shown to be resistant to the PERK-mediated cell-cycle arrest.

Intriguingly, the translational repression occurring through PERK activity is also responsible for the translational upregulation of a specific transcription factor termed ATF4, and the subsequent transcriptional induction of some UPR target genes [54,55]. This pathway is similar to yeast and mammals signalling cascades activated in response to amino acid starvation, in which the eIF2α kinase Gnc2p promotes the translation of GNC4 (ATF4). The transcription factor ATF4 was shown to upregulate the transcription of CHOP gene encoding the C/EBP homologous protein-10 (CHOP), which is a transcription factor that promotes cellular apoptosis [54,56]. Interestingly, PERK signalling has also been linked to the upregulation other genes such Bip and GADD 34 (growth arrest and DNA damage), but the role of ATF4 in these events is still unclear [55,57]. GADD34 protein promotes the dephosphorylation of eIF2a by binding to the catalytic

subunit of protein phosphatase1 (PP1) thereby providing a negative feedback loop to the stress response [57].

2.3-UPR and the upregulation of ERAD

ERAD is a process naturally occurring in a non-stressed cell by which misfolded or misassembled retrotranslocated to the cytosol through the Sec61 channel and subsequently degraded by the proteasome [58]. As mentioned earlier, studies on the QCM demonstrated that the targeting of misfolded N-glycosylated proteins to the Sec61 channel involves the CNX cycle [59]. The targeting of proteins to retrotranslocation has also been associated with the chaperone Bip [60]. However, the mechanism of protein retrotranslocation remains poorly understood.

The regulatory link between UPR and ERAD emerged from genetic studies performed in yeast, where cells bearing mutations in ERAD-mediating genes were shown to grow normally through the induction of UPR [61]. In addition, genomic analysis demonstrated that the UPR mediates the upregulation of genes directly involved in ERAD and ubiquitin system along with many other genes involved in translocation, protein folding and protein glycosylation [62]. Since ERAD uses the proteolytic components of the classical ubiquitin/proteasome pathway, the processing of retrotranslocated proteins on the cytosolic side of the ER has been characterized in greater details [63].

The first step in the degradation of proteins associated with ERAD involves Hrd1p, which is an ER integral membrane protein of the E3 family of ubiquitin-protein ligases [64]. Hrd1p designates the E2 ubiquitin-conjugating enzyme that will transfer multiple copies of the small protein ubiquitin to the retrotranslocated proteins in order to target them to degradation by the proteasome. During yeast and mammalian ERAD, the principal E2 involved in Hrd1-dependent protein degradation is Ubc7, which requires an integral ER membrane protein termed Cue1 to be recruited to the lipid bilayer [60,61]. In the yeast, Ubc1p and Ubc6p have also been reported to act on ERAD substrate [60,63]. In at least some cases, ERAD depends on two integral membrane proteins, namely Hrd3p and Der1p, which have not yet been assigned a clear function.

2.4-UPR and apoptosis

The UPR outputs in the mammalian cells have profound consequences on the global cellular signalling activities. Depending on the intensity, the duration and the nature of the ER stress suffered by the cell, the UPR will encourage cell survival or induce apoptosis [18]. Indeed, ER-stress inducers such as tunicamycin (Tun), which blocks N-linked protein glycosylation, dithiothreitol (DTT), which impairs the formation of disulphide bonds, brefeldin A, which inhibits ER-Golgi transport, and thapsigargin, an agent inducing UPR by depletion of the luminal calcium stores are all known to induce cell death [65]. However, it should be noticed that induction of apoptosis is not common to all UPR activators. As mentioned above, CHOP is one of the first UPR-related apoptotic effectors identified; the expression this member of the C/EBP family of transcription factors was first related to other metabolic stresses [56]. Elevated levels of CHOP protein result in the down-regulation of the expression of Bcl2 and in the depletion of cellular glutathione, which is the primary intracellular scavenger of reactive oxygen species (ROS) [66]. Since Bcl2 is a molecule having anti-apoptotic functions and that exaggerated ROS production results in the disruption of the cellular redox homeostasis, elevated CHOP expression readies cells for apoptosis. Even if CHOP sensitizes cell to ER stress inducers, the protein is not alone sufficient to trigger apoptosis [65,66]. It is interesting to add that the transcription activator function of CHOP through phosphorylation of the protein by p38, which is a stress-responsive protein kinase of the mitogen-activated protein kinase (MAPK) family [67].

Another major local factor in the ER-induced apoptosis is the cysteines protease termed caspase-12 [68]. Caspase-12 is a member of the interleukin-1β converting enzymes (ICEs) that facilitates apoptosis in cell irreversibly damaged by endoplasmic reticulum stress [69]. The exact mechanism of action of caspase-12 in apoptosis is still unclear, but significant progresses have been made lately in identifying the molecules involved in its activation. Indeed, UPR was hypothesized to trigger the cleavage of procaspase-12, which is the inactive form of the caspase, through the activation of Ire1s and the adaptor molecule tumor necrosis factor receptor-associated factor 2 (TRAF2) [70]. TRAF2 is known to form a stable complex with procaspase-12 in unstressed cells and to associate with Ire1 during the UPR. ER stress was demonstrated to trigger the dissociation of

procaspase-12 from TRAF2, which allows a simultaneous dimerization (or oligomerization) of procaspase-12. Since procaspases such as caspase-2, -8 and –10 can be activated through dimerization/oligomerization, a similar mechanism has been suggested for procaspase-12 activation [69]. However, a recent study proposed a calcium-induced activation of the molecule, which would involve the cleavage of procaspase12 by the cysteine protease termed calpain [71]. Since JNK inhibitory kinase (JIK) promotes the interaction Ire1s with TRAF2, a role of JIK/TRAF2 signalling complex has also been suggested for the activation of caspase-12 [70]. It is important to add that Ire1s/TRAF2 and Ire1s/JIK/TRAF2 complexes were independently demonstrated to be involved in the UPR-induced activation of the c-Jun amino-terminal kinase (JNK), which belong to a family of stress-activated kinases related to apoptosis signalling [72,70].

The ER-mediated apoptosis could also involve the initiator caspase-8, which is activated in signalling pathways downstream of death receptors at the plasma membrane [69]. Indeed, a regulation of the caspase-8 activity has been suggested for Bap31, which is an ER-enriched multispanning transmembrane protein [73]. The cytosolic portion of Bap31 can associate with pro-caspase8 and a Bcl-2/BclX_L complex through a Ced-4-like adaptor molecule [74]. Ced-4 molecule was identified in C.elegans, where it is involved in the regulation of apoptotic programmed cell death. The association of Ced-4 with Ced-9, which is the Bcl-2 homolog in the nematode, prevents Ced-4 from activating the caspase Ced-3 [75].

Recently, two identical caspase cleavage sites were identified in Bap31 cytosolic portion. The C-terminal site can be processed by either caspase8 or caspase 1 in response to various death stimuli including some ER stress inducers [76]. The soluble fragment generated was shown to impair the anterograde transport from the ER to the Golgi when ectopically expressed, which could account for some of the alterations observed in dying cells. Moreover, the resulting membrane-integrated fragment of Bap31, called p20, is a potent inducer of apoptosis when expressed ectopically, suggesting that Bap31 cleavage may contribute in different ways to the death process [77]. Even if an interaction of Bap31 with CNX has recently been detected [78], the exact mechanism responsible for Bap31

activation upon ER stress and the exact contribution of Bap31 in the ER-induced apoptosis are still poorly understood.

3-The endoplasmic reticulum overload response (EOR)

Overexpression of wild-type viral proteins causes an accumulation of protein in the ER that has no effect on the UPR pathway [6]. Instead, this type of ER stress activates the transcription factor NF-κB, which induces the transcription of pro-inflammatory and immune response genes [79]. This signalling pathway was named endoplasmic reticulum overload response (EOR). Although several drugs inducing protein misfolding or ER store Ca++ depletion activate UPR and EOR, it is possible to distinguish between the UPR and EOR by pharmacological intervention [18]. Indeed, the phosphatase inhibitor okadaic acid potently induces NK-κB, whereas it has not significant effect on UPR induction [18,80].

NF-κB is a heterodimer present in the cytoplasm in an inactive complex with IκB, the inhibitor of NF-κB [81]. Exposure of cells to a number of stress inducers induces the phosphorylation of IκB, which is subsequently targeted for ubiquitination and degradation by the proteasome. Released NF-κB heterodimer translocates to the nucleus and activates target genes. NK-κB functions are assumed to protect cells from apoptosis, and a recent publication demonstrated that NF-κB represses the expression of CHOP during ER-stress [82]. The EOR appear to induce NF-κB through the ER-mediated Ca++ release and the subsequent generation of reactive oxygen intermediates (ROIs) [83]. Although ER-localized peroxidase activities are suggested to be important for the Ca++-dependent activation of NF-κB, the role of ROI in this process is still a mater of debate [83,6]. However, the importance of Ca++ signalling for the activation of NF-κB during the EOR has been firmly established [83,84]. Although the characterization of the mechanism by which Ca++ signalling activates NF-κB awaits further investigations, recent progress has been made in understanding how the accumulation of proteins could stimulate Ca++ release.

A recent publication suggested that CNX/CRT participate directly in the $[Ca^{2+}]_l$ regulation through their inhibitory interaction with the Ca ++ pump SERCA2b [85].

While the binding of CRT to SERCA2b relies on the N-glycosylation of SERCA2b at Asn1086, the inhibitory interaction of CNX with the Ca++ pump requires the phosphorylation of CNX cytosolic tail at Ser562. The de-phosphorylation of this residue is Ca++-sensitive [85] and hyperphosphorylated CNX is observed following okadaic acid treatment [86]. Furthermore, the extracellular-regulated kinase 1 (ERK1) was shown to mediate the phosphorylation of CNX at Ser562, thereby promoting the association of CNX with ribosomes [87]. This mechanism is suggested to enhance CNX presence near the translocon to increase the productive folding of nascent N-glycosylated protein. Since it was established that Ca++ modulates the functions of the Ca++-binding chaperone CRT and CNX [4], they could act as Ca++-regulated stress sensing molecules. In fact, CRT-deficient cells are significantly resistant to apoptosis induced by ER stressors while a sensitization to the latter is observed in cells overexpressing CRT [88]. It is also interesting to note that SERCA2b gene expression is induced by ER stress, and that ATF6 regulates the SERCA2 gene expression during ER stress in cardiac myocytes [89,90].

The Ca++ signalling may explain how a stimulus can activate UPR and EOR, but recent evidences suggest that these pathways also share signalling molecules. Indeed, TRAF2 was shown to activate NF-κB in response to some ER stress inducers and the implication of Ire1 has been proposed [91]. This signalling cascade would be involved in adaptation and survival as opposed to the JNK pathway associated to apoptosis. However, it raises a controversy about the qualification of UPR and EOR as being distinct signalling responses.

4-The endoplasmic reticulum stress and the MAPK family

Depending on the nature, the strength and the length of the stress stimulus, as well as the environment to which it is confronted, the cell will either adapt or die by apoptosis. Determination of life and death in response to stresses is known depend on the balance of intrinsic life and death signals generated within cells [65]. Part of this signalling occurs via the mitogen-activated protein kinases (MAPKs) family of Ser/Thr protein kinases [92]. MAPKs family can be divided into two categories, the kinases involved in survival signalling and the stress-activated MAP kinases (SAPKs), which are usually implicated in

apoptosis signalling [93]. The first category is constituted by the two isoforms of the extracellular-regulated protein kinase (ERK) termed ERK-1 and ERK-2. Among the members of the SAPKs, two kinases subfamilies have been characterized in some details: c-Jun N-terminal kinases family (JNKs) and the p38 MAPKs family. All these kinases are structurally similar and the hierarchy of their signalling cascade is conserved from yeast to mammals [94].

The typical ERK signalling pathway begins with the activation of a receptor tyrosine kinase (RTK) at the plasma membrane (PM) by a mitogen or a growth factor, which induce the dimerization and the trans-autophosphorylation of the receptor [94]. Activated RTK recruits the guanosine nucleotide exchange factor (GEF) SOS via adaptor proteins such as Shc and/or GRB2, which allows the activation of the small guanosine triphosphatase (GTPase) Ras at the PM. Ras activates the MAPK kinase kinase (MAPKKK) Raf, which is a Ser/Thr protein kinase that phosphorylates and activates the MAPK kinase (MAPKK) MEK. This Ser/Thr protein kinase subsequently phosphorylates and activates ERK (also referred to as MAPK), which translocate to the nucleus and activates the transcription factor Elk-1 inducing gene expression related to cell growth, differentiation, mitosis or survival [92].

The JNK subfamily of SAPKs is composed of three genes (jnk1, jnk2, and jnk3) from which alternative splicing can produce ten isoforms that are activated by two distinct MAPKKs termed MKK4/SEK1 [93]. JNKs phosphorylate the transcription factor cJun leading to the upregulation of genes with AP-1 sites in their promoter region. Even if cJun is the primary target of JNKs, they can activate several other transcription factors including Elk-1, ATF-2, PEA3 and Sap-1a. The p38 subfamily includes five members termed p38α, p38β, p38γ, SAPK3 and SAPK4, which are activated by two different MAPKKs namely MKK3 and MKK6 [93]. The primary target of p38s is the transcription factor ATF-2, but they also phosphorylate and activate other transcription factors such as Sap-1a and CHOP/GADD153.

The MAPKKKs involved in SAPKs activation are highly divergent in structure, gene number and the specificity of their activation. For instance, eleven different MAPKKKs responsible for JNKs activation have been identified so far. Of these, five kinases also

activate the ERKs, while three other have been shown to activate p38s (reviewed in [92]). To add even more to this level of complexity, at least 14 different but structurally related kinases are suggested to function upstream of MAPKKKs in the SAPKs pathways. Despite the lack of direct biochemical evidence that these kinases activate MAPKKKs by phosphorylation, they have been termed MAPK kinase kinase kinases (MAPKKKKs). Overall, the cells may utilize this diversity of kinases upstream of SAPKs to discriminate and differentially respond to the wide variety of extracellular stimuli and physicochemical stressors [(93)].

Several signalling molecules associated with the activation of a different type of receptor protein at the plasma membrane are involved in the activation of the SAPKs upstream of the MAPKKKs and the MAPKKKKs. For instance, tumor necrosis factor receptors (TNFRs) family activate the SAPKs through TRAF2, TRAF5 or TRAF6 [(95)]. The superfamily of small GTPases is also thought to play an important role in the activation of the SAPKs. Rac and Cdc42, two members of the Rho family of small GTPases, are known to activate JNKs and p38s following different cellular stresses [(96)]. Although the exact mechanism of this activation remains unclear, it may require MAPKKKK such as PAK [(97)]. Since activated Ras can lead to the activation of Rac and other small GTPases, cross talks between ERK signalling cascade and SAPKs pathways may lead to the activation of JNKs and p38s [(98)].

The signalling events stimulated by epidermal growth factor (EGF) are a good example of cross talk between MAPK/SAPKs signalling cascades. Activated EGF receptor (EGFR) recruits the adaptor Grb2 through its SH2 domain, which allows the translocation of SOS and the activation of Ras/ERK cascade [(94)]. Conversely, the activation of JNK by EGF is dependent on the adaptor Shc but not Grb2 [(99)]. Shc contains a phosphotyrosine-binding domain (PTP) and an SH2 domain, which mediate the association with RTKs. The SH2 domain of Shc is responsible for the recruitment to activated EGFR and was implicated in the EGF-mediated activation of Shc by tyrosine phosphorylation [(100)]. The role of Shc in the EGF-induced activation of JNK is related to the formation of a complex with Grb2, which would either activate Ras (and subsequently Rac) or recruit a GEF for Rac/Cdc42 such as Vav [(99-101)].

The activation of SAPK downstream of activated EGFR could also be related to Nck adaptor, which contains three SH3 domains and one SH2 domain [102]. Although Nck interaction with EGFR is not direct, the SH2 domain is activated by tyrosine phosphorylation when recruited near EGFR. Activated Nck has been demonstrated to activate the JNK cascade through Rho GTPases-dependent and -independent mechanisms. The first involves the interaction of Nck with members of the family of p21-activated Ser/Thr kinases (PAKs) through Nck mid-SH3 domain [103]. The recruitment of Nck-PAK1 or -PAK3 complexes to the plasma membrane activates Rac and Cdc42, which lead to the activation of JNK and p38 pathway [97]. The small GTPases-independent mechanism rely on the interaction of Nck with the Nck-interacting kinase (NIK) via Nck middle and C-terminal SH3 domains of Nck [104]. NIK binds to and activates MEKK1, which is a MAPKKK leading to the upregulation of JNK activity.

As exposed earlier, the MAPK family is involved in the ER signalling; the functions of CHOP and CNX are respectively regulated by p38 and ERK, and the UPR activates JNK. Although, the mechanism of activation and the functions of MAPK/SAPKs during ER stress are still poorly understood, recent publications illustrated intriguing feature of the ER in the regulation and in the synthesis of signalling molecules of the MAPK/SAPKs pathways. Indeed, the ER-anchored phosphotyrosine phosphatase 1B (PTP1B), is mediating the dephosphorylation of many endocytosed RTKs including EGFR [105]. Since the synthesis, the signal termination and the recycling/degradation of RTKs are associated with a transit through different ER sub-compartments, some aspect of the ER signalling machinery may be intimately associated with the RTKs signalling.

In the same line of evidence, an important pool of Shc proteins is associated with the cytosolic side of the RER in unstimulated cells [106], raising the possibility that Shc may be involved in signalling events occurring at ER. EGF treatment induces the redistribution of Shc to the plasma membrane and endocytic structures trough a mechanism independent of Shc phosphorylation [106]. Another intriguing feature of the ER concerns the prenylation and the anchoring of small GTPases of the Ras family occurring at the cytosolic side of the ER. Recent publications demonstrated that the

consensus site for prenylation, the CAAX motif, targets these proteins to the ER and Golgi membranes [107,108]. Furthermore, many enzymes involved in the different steps of the prenylation are localized at cytosolic side of ER and Golgi, and they are suggested to regulate the flux of Ras family members to the plasma membrane [109,110]. Unfortunately, the activities of these small GTPases present on the ER/Golgi have not been assessed. In conclusion, the remarks presented above suggest that the ER may have important functions in the regulation of the MAPK/SAPKs pathways and that the ER stress could influence the interactions between ER and these cascades.

Goals and hypothesis

This work aims the development of a new method to study the ER signalling in response to drugs inducing protein misfolding. We hypothesize that the ER signalling could be reconstituted in a cell free system using magnetic ER compartments isolated with beads coated with antibodies for calnexin. We theorize that the ER signalling activates ERK-1, JNK-1 and p38 in response to treatments with AZC, DTT and Tun, which induce ER stress. We also hypothesize that the modulation of these kinases by the ER signalling could occur through Shc and Nck adaptor proteins.

We report here the immunoisolation with anti-CNX-coated magnetic beads of ER-like compartments that can be used in a cell free system to reproduce the ER signaling through kinase phosphorylation and kinase activity assays. We show that this compartment contains per se the information required for the activation of MAPK/SAPKs in response to stress. Indeed, we demonstrate that the CNX-enriched compartment is mediating the activation of ERK-1, JNK-1 and p38 upon AZC treatment and that Tun induces an ER-mediated activation of JNK-1 and p38. We observe that the cell free assays can be perturbed by the addition of GST constructs for Shc and Nck or the depletion of these adaptors from the cytosol added to the assays. We provide further evidences for the involvement of Shc and Nck in the ER signalling through microsomes phosphorylation assays.

Experimental procedures

Materials

Anti-Calnexin is a polyclonal antibodies raised against a synthetic peptide (C4: residues 555-573) as described in Ou et al. (1993). Anti-MG-160 was kindly provided by Dr. N. Gonatas (University of Pennsylvania, Medical Center, Phidadelphia, PA). Anti-Tom-20 was a generous gift from Dr. G. Shore (McGill University, Montreal, PQ). Anti-ERK-1 (K-23), anti-JNK-1 (C-17) and anti-p38 (C-20) were purchased from Santa-Cruz Biotechnologies (Santa-Cruz, CA). Anti-EGFR is a polyclonal antibodies raised against a synthetic peptide (residues 1164-1176) as described in Wada et al. (1992). Anti Nck antibodies and GST fusion protein of ATF2, Shc and Nck were kindly provided by Dr. Louise Larose (McGill University, Montreal, PQ). GST fusion protein of c-Jun and Anti-Shc antibodies was a generous gift of Dr. Tony Pawson (University of Toronto, Ontario). All other lab products were purchased from Sigma Chemical Company (Oakville, OT), Boehringer Mannheim (Laval, PQ), Fisher Scientific (Nepean, OT) and Anachemia (Lachine, PQ) unless specified otherwise.

Analysis of FR3T3 cells ER membranes on a linear sucrose gradient

Two dishes of 70% to 80% confluent FR3T3 cells were scraped in a buffer containing 0.25 M sucrose, 4 mM imidazole pH 7.4, 1 mM PMSF, 1 μg/ml leupeptin, 1μg/ml aprotinin. The cells were then homogenized with 30 strokes of motor driven Potter homogenizer. Post-nuclear supernatant was obtained after a 1500 g spin and was loaded on a linear sucrose gradient (d1.05-d1.25) done in a plastic ultracentrifuge tube by mixing a 2.2M sucrose, 4mM immidazol pH7,4 solution with a 0,5M sucrose, 4mM immidazol pH7,4 solution using a pump and tubing. Separation on the sucrose gradient was accomplished at 4°C through a 17h spin at 25000 rpm (Beckman SW40). Fractions were collected every 30 sec using a pump and tubing. Fractions were precipitated with the addition of a half volume of tri-carboxylic acid (TCA) 20%. After 15 min. incubation at 4°C, samples were centrifuge for 5 min. at max speed in a microfuge; the supernatant was discarded and the tubes re-centrifuged following the same conditions. The protein pellets

were resuspended in a 70% ethanol solution at –20°C overnight. Samples were analysed by 10% SDS-PAGE and immunoblot with anti-CNX antibodies.

Cell culture and immunopurification of the ER-like membranes

FR3T3 were cultured in Dubecco's modified Eagle medium (DMEM) (GIBCO) supplemented with 10% foetal bovine serum (FBS) (Hyclone, Logan, UT). They were maintained at 37°C in an incubator with a 5% CO_2 containing atmosphere. Cells were passed every 3 days and were used at 70 to 90% confluence. The 10 min. drug treatments were done on cells serum starved for 1h, with 10 µg/ml Tunicamycin (Roche) 10 mM Azetidine 2-carboxylic acid (AZC), 2 mM dithiothreitol (DTT), and 50 mM Sodium arsenite. Cells were then washed once in PBS solution and once in homogenization buffer containing 30 mM Tris-HCl pH 8.0, 150 mM NaCl, 1 mM phenylmethylsolfoninyl fluoride (PMSF) 1 µg/ml leupeptin and 5 KIU/ml aprotinin (buffer A). Cells were then homogenized with 30 strokes of motor driven Potter homogenizer. Post-nuclear supernatant was obtained after a 1500 g spin using a Sorvall centrifuge with an ss-34 rotor. M450 magnetic beads (Dynal Biotech) were cross-linked with the anti-CNX-C4 antibody at 37°C for 90 min according to the manufacturer's instructions. Antibody-coated magnetic beads were incubated with membranes in buffer A, to which 0,5 mg/ml of milk powder was added, for 2h in the cold room with gentle agitation. Beads were then isolated with a magnet and washed repeatedly in buffer A. The quality of the isolated membranes was assessed by immunoblotting and electron microscopy analysis. The same procedure was used for the purification of plasma membrane, but the magnetic beads were coated with Wheat Germ Agglutinin (WGA).

SDS-PAGE analysis

Samples were boiled in Leammli buffer for 5 minutes and centrifuged at max speed in a microfuge. Samples were separated by either 10% or 12.5% SDS-PAGE and transferred onto a nitrocellulose membrane at 12V for 90 minutes at 4°C in a buffer containing 192 mM glycine, 25mM Tris. Alternatively, some gels were stained with coomassie blue (0.1% Coomassie blue R250 in 50% methanol and 10% glacial acetic acid), destained (30% methanol, 7% glacial acetic acid) and dried for 2h at 80°C under vacuum.

Transferred blots were incubated in a blocking solution (PBS 1X, 0.05% Tween, 5% dried milk) for 1h at room temperature. The blots were incubated with gentle agitation with given antibodies in a blocking solution containing only 0.5% dried milk for 1h at room temperature or overnight at 4°C. After four successive 10 to 15 min. washes with a solution containing PBS 1X and 0.05% Tween, blots were incubated with the appropriate secondary antibodies conjugated to HRP which are diluted in a blocking solution as described above. After four other successive washes, a chemiluminescence reaction was performed as described by the manufacturer. Visualization of immunoblot was done by exposure to Kodak X-OMAT films at room temperature. Autoradiography was performed on dried gel or nitrocellulose membranes by exposure to Kodak Biomax films at –80°C with a Kodak enhancing screen. Densitometry analysis was performed using a Bio-Rad analyzer and software as described by the manufacturer.

Electron microscopy

Immunopurified membranes were fixed for 2.5h with 2.5% gluteraldehyde in 0.1 cacodylate buffer containing 0.05% calcium chloride pH 7.4. Samples were then filtered onto a 0.45 μM pore size filters and washed with 0.1M cacodylate buffer overnight. Samples were then treated with a 1:1 solution of 3% potassium ferrocyanide and 2% asmium tetroxide for 1h on ice, washed with 0.1 M maleate buffer pH 5.7 and stained with 5% uranyl acetate for 2h on ice. After two washes with 0.1 maleate buffer and one with 0.1 cacodylate buffer, samples were dehydrated with a graded series of ethanol washes followed by a 100% propylene oxide wash. Samples were placed in a 1:3 mixture of Epon and propylene oxide for 1h, followed by incubation in a 1:1 mixture for 1h, then 100% Epon for 1h. Samples were placed in a 60oC oven for polymerization. Thin sections were cut, stained for 2 min. in lead citrate and 5 min. in uranyl acetate. Micrographs were taken at a 37500 magnification on a JOEL JEM-2000FX electron microscope (Philipps 400) operating at 80.0 kV and prints were magnified a further 1.8X.

Cell-free assays

For each assay, 30 μg of immunopurified membranes were incubated with 3mg of rat liver cytosol for 30 min. at 30°C in a buffer containing 30 mM Tris-HCl pH 8.0, 10 mM

$MgCl_2$, 1mM NaF, 1mM Na_3VO_4, and 0.1 mM ATP with or without 10μCi [$^{32}P\gamma$]-ATP; the isolation of rat liver cytosol is described in the cellular fractionation section. The reaction was stopped by the addition of 4 mM ATP (final concentration). Membranes were collected with the magnet and the remaining fragments spun down at 100 000 rpm for 20 min. in a Beckman TLA-100.2 rotor or at 14 000 rpm for 20 min. in a microfuge. Triton X-100 was added to the supernatants (1% final concentration). ERK-1, p38 and JNK-1 were then immunoprecipitated (2h at 4°C) and their phosphorylation state was analysed by autoradiography and western blotting after an SDS-PAGE separation and transfer onto a nitrocellulose membrane. In parallel, kinase activities were measured by in vitro phosphorylation of 2 μg Myelin Basic Protein (for ERK-1), 2 μg GST-ATF2 (for p38) or 2 μg GST-cJun (for JNK-1); the reaction was stopped by adding 2X Laemmli buffer and boiling. The kinase phosphorylation assays were also performed with reaction buffers containing 10 μg of GST, 5 μg of GST-Nck-$SH3_1$ + 5 μg of GST-Nck-$SH3_2$ or 10 μg of GST-Shc-SH2 as well as with rat liver cytosol depleted in Shc or Nck. The depletion of Shc or Nck adaptors, which was followed by western blot analysis, required two successive immunoprecipitations with their respective antibodies. The kinase phosphorylation assays performed with WGA-purified plasma membrane-like compartments were executed as just described.

Cellular fractionation

Male rats were treated for 18h with Tunicamycin, 1μg/gr. of body weight in PBS solution, by intraperitoneal injection. Animal were then anaesthetized and killed by decapitation. After blood draining, the liver was removed from the animal and placed in an ice-cold homogenization buffer (buffer B: 0.25 M sucrose, 4 mM imidazole pH 7.4, 1 mM PMSF, 1 mM NaF, 1 mM Na_3VO_4). Liver was then rinsed, minced with a razor blade or scissors and homogenized in the buffer B (20% w/v) with 5 strokes of motor-driven Potter-Elvejham homogeniser set at 2300 rpm. The homogenate was centrifuged at 3100 rpm (Sorval ss-34) for 10 min. The resulting post-nuclear supernatant was decanted and centrifuged at 6000 rpm (Sorval ss-34) for 10 min., and the supernatant was removed and kept on ice. The pellet was re-homogenized in half volume of buffer B with one stroke of Potter and re-centrifuged at 6000 rpm. The supernatants were pooled and

centrifuged at 25 000 rpm (Beckman Ti60) for 6 min. 40 sec. The resulting supernatant was removed and kept on ice while the pellet was resuspended in ½ volume of buffer B and re-centrifuged as described above. The supernatants were pooled and centrifuged at 45 000 rpm (Beckman Ti60) for 40 min. The resulting supernatant (cytosol) was removed and the pellet was resuspended in 1.5 ml of buffer B per gram of liver. This solution was placed on a discontinuous sucrose gradient made of 3 ml of 1M, 1.2 M and 1.38 M sucrose, and centrifuged at 40 000 rpm (Beckman SW40) for 3h. The smooth microsomes are collected at the interface of 1.2M/1.38M and the pellet is constituted by the rough microsomes.

Microsomes phosphorylation assays

For each assay, 100µg of microsomes were diluted with distilled water and stock solutions to obtain a 100µl reaction mix containing 30 mM Tris-HCl pH 8.0, 10 mM $MgCl_2$, 1mM NaF and 1mM Na_3VO_4, 0.1 mM ATP and 20 µCi [$^{32}P\gamma$]-ATP The phosphorylation reactions were performed on ice for 30 min. and stopped by boiling during 5 to 10 min. The volume of the samples were adjusted to 1 ml with a lysis buffer to achieve 30 mM Tris-HCl pH 8.0, 150 mM NaCl, 1 mM PMSF, 1 µg/ml leupeptin, 5 KIU/ml aprotinin and 1% Triton X-100. The samples were incubated with antibodies for Shc or Nck at 4°C for 2h, and the immunoprecipitates were resolved by SDS-PAGE. Phosphorylated Shc and Nck were visualized after gel drying and exposure to Kodak Biomax films.

Results

Immuno-isolation and characterization of an ER-like compartment

One of the problems occurring during the study of the impact of ER signalling on cytosolic kinases is to ensure that the events observed are really triggered by the ER. Several methods have been developed over the years to isolate biological membranes related to the ER. Unfortunately, most of these methods are based on typical subcellular fractionation that isolate ER-like membranes with a non-negligible contamination by plasma membrane (PM), Golgi and mitochondria [111]. Moreover, the procedure used to further purify the membranes strip proteins adsorbed on their cytosolic side [111,112]. Recently, a new method was developed to isolate peroxisomes [113] or Golgi [114] with a high degree of purity. This method rely on the used of magnetic beads to which antibodies or proteins have been covalently bound. The epoxy groups covalently bound at the surface of the beads form covalent bounds to primary amino groups in proteins and peptides following 90 min incubation at 37°C. The protein or the antibody used to coat the magnetic bead should be selected for its property to interact with the membrane of the studied organelle. After an appropriate incubation of the cellular homogenate with the beads, the given organelle is gently pulled down using an ependorff-shaped magnet. We decided to adapt this new method to isolate an ER-like compartment from drug-treated FR3T3 fibroblast cell line since fibroblasts are commonly used in ER signalling research [18,82].

Results previously published by our group suggested that CNX is one of the most abundant proteins of the ER [115]. Since CNX is a transmembrane protein and that our group developed a very good polyclonal antibody to CNX cytosolic tail [116], this antibody was a good candidate for the coating of magnetic beads. However, we wanted to ensure that CNX distribution on ER membrane was broad enough to ensure the proper isolation of the organelle. Consequently, the microsomal membranes of FR3T3 cells were analysed on a linear sucrose gradient where the density was adjusted for the analysis of high-density and low-density ER fractions, which represent rough and smooth ER respectively. After TCA precipitation, the protein content of these fractions was analysed

on SDS-PAGE and immunoblotted with CNX antibodies. The wide distribution of CNX in both high-density and low-density fractions can be observed in figure 1. Even if CNX seems to be absent in the microsomal membranes with the lowest and the highest density, we decided to use CNX antibody to coat the magnetic beads used in the immuno-isolation experiment depicted in figure 2.

The membranes isolated with the magnetic beads presented a relatively high degree of purity as demonstrated by the biochemical analysis presented on figure 3. Both crude homogenate and the ER-like compartment were analysed by SDS-PAGE and immunoblotted for CNX (ER marker) [115], EGFR (PM marker) [99], Mg-160 (Golgi marker) [117], and Tom 20 (mitochondrial marker) [118]. By comparing the crude homogenate to the ER-like membranes, enrichment in ER/CNX by approximately 15 fold can be observed. The immuno-isolated membranes are practically devoid of PM and Golgi contaminants, but a slight mitochondrial contamination is visible. We pushed further the analysis of the ER-like compartment purity by performing an electron microscopy analysis where the magnetic beads were used as solid support. The electron microscopy pictured in figure 4 revealed a large ribosome-containing ER compartment tightly associated with a mitochondrion.

Figure 1

Western blot analysis of cell fractionation on linear sucrose gradient

FR3T3 homogenate supernatant is separated on linear sucrose gradient (d1.05-1.25) as described in Experimental procedures. Corresponding fractions were separated by 10% SDS-PAGE, transferred onto a nitrocellulose membrane and immunoblotted for CNX. The figure indicates the distribution of CNX in high-density and low-density fractions of the ER.

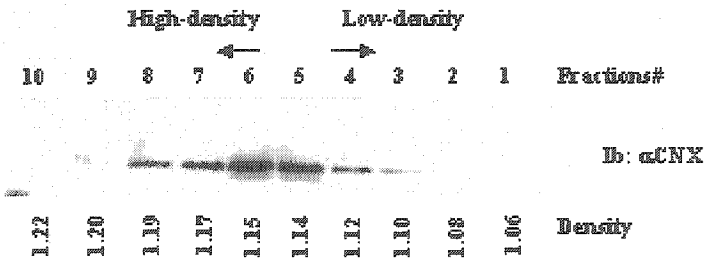
High-density
Low-density
10 9 8 7 6 5 4 3 2 1
Fractions#
Ib: αCNX
1.22 1.20 1.19 1.17 1.15 1.14 1.12 1.10 1.08 1.06
Density

Figure 2

Scheme of the experimental procedure used to immunopurify an ER-like compartment

Drug treated FR3T3 cells were homogenized and the ER-like CNX containing compartments were isolated using anti-CNX antibodies-coated magnetic beads as described in the Experimental procedures section.

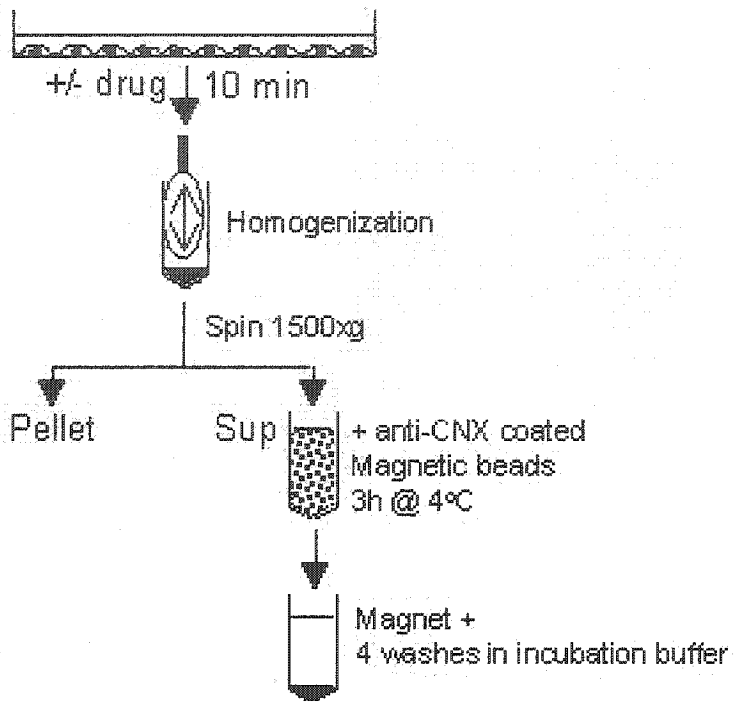
+/- drug
10 min
Homogenization
Spin 1500xg
Pellet
Sup
+ anti-CNX coated
Magnetic beads
3h @ 4°C
Magnet +
4 washes in incubation buffer

Figure 3

Biochemical analysis of the immunopurified membranes

The same amount of total proteins corresponding to either ten percents of the post-nuclear membranes (lane 1) or the total immunopurified ER-like compartment (lane 2) were separated by 12.5% SDS-PAGE, transferred onto a nitrocellulose membrane and immunoblotted with anti-CNX (endoplasmic reticulum marker), anti-EGFR (plasma membrane marker), anti-MG-160 (Golgi marker) and anti-Tom20 (mitochondrial marker).

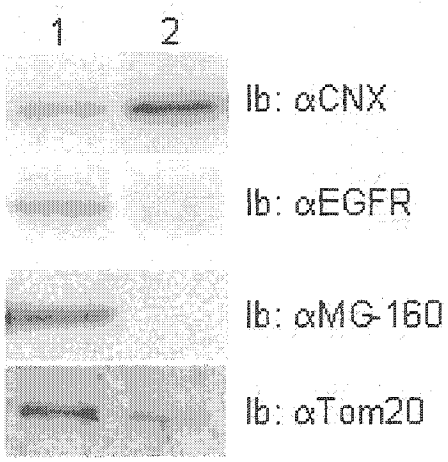
1
2
Ib: αCNX
Ib: αEGFR
Ib: αMG-160
Ib: αTom20

Figure 4

Electron microscopy of the immunopurified compartment

Electron microscopy was performed on freshly immunopurified membranes as described in Experimental procedures. Endoplasmic reticulum-like membranes (ER) with ribosomes (R) as well as a mitochondria (M) and magnetic beads (B) are indicated on the picture. Magnification bar represents 0.5μm.

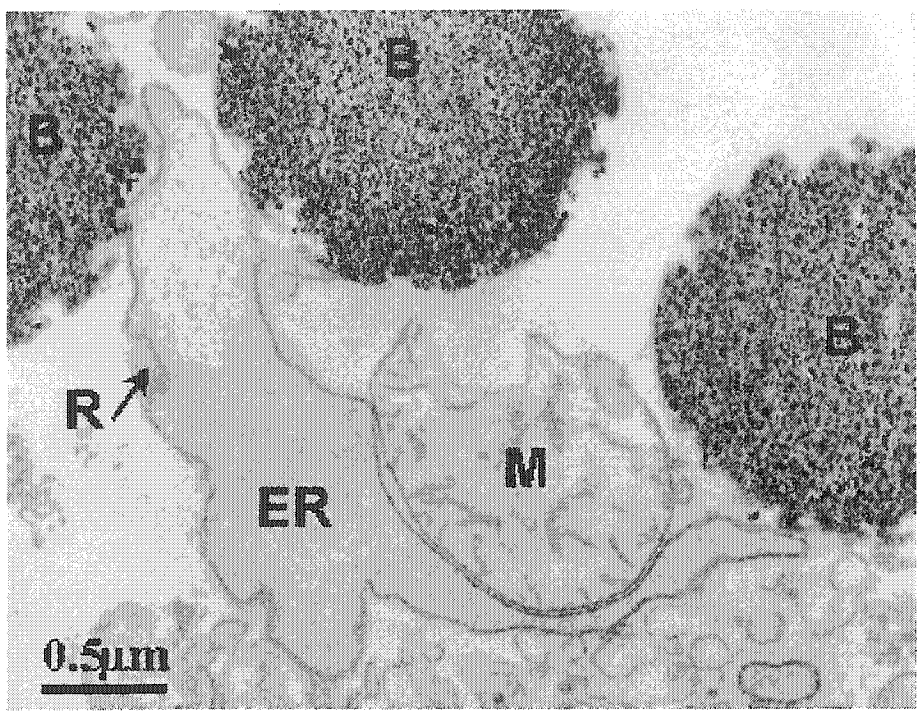
B
B
B
R
M
ER
0.5µm

Cell-free reconstitution of the ER-mediated activation of MAPK and SAPKs

We treated fibroblasts with four different drugs to study the ER signalling. AZC, DTT, and Tun were chosen because they specifically induce ER stress while sodium arsenite (NaAs) was selected as a control since the cellular stress induced by this drug does not involve ER signalling[119]. As discussed in the literature review section, AZC is a proline analogue that impairs the correct folding of proteins when incorporated in their amino acid sequence; DTT is a chemical disrupting the disulphide bonds of proteins, and Tun is a drug impairing proper folding of N-glycosylated proteins by inhibiting their N-glycosylation [18]. NaAs impairs the cellular respiration by forming a complex with vicinal dithiols of lipoamide-containing enzymes [1,9]. However, short exposure to a low concentration of this drug was shown to trigger misfolding of cytoplasmic proteins but to have no effects on proteins located inside the ER [119]. All these drugs, but not AZC, also possess the ability to induce apoptosis at different intensities [65,18]. We thus hypothesized that the drugs used to induce ER stress would activate with different strength the stress-activated kinases JNK-1 and p38, which are normally associated with apoptosis signalling [92]. We also presumed that these drugs could activate ERK-1 given that the relatively short length of the drug treatments may allow survival messages within the cells.

To study the effects of ER stress on the activity of the MAPK and SAPK, we developed cell free assays where ER-like membranes immuno-isolated from drug-treated cells are incubated with rat liver cytosol, which is an adequate source of kinases. For a given drug treatment, the ER-like compartments isolated were divided into two samples. The first was used for the kinase phosphorylation assay, in which the membranes are incubated with cytosol and P^{32} labelled ATP. The second sample was used for the kinase activity assay, in which the reaction involving the membranes and the cytosol is carried out with non-labelled ATP. While in the first assay the kinases studied are immunoprecipitated and directly analysed by SDS-PAGE, the second assay contained an extra step where the immunoprecipitated kinases are incubated with specific substrates and ATP^{32}. A scheme of these experimental procedures is illustrated in the figure 5.

We first studied the modulation of ERK-1 activity following the different drug treatment. The SDS-PAGE analysis of ERK-1 immunoprecipitated from kinase phosphorylation assays was transferred onto a nitrocellulose membrane, which was subjected to autoradiography and to a western blot analysis for ERK-1 that ensured that the same amount of kinase was present in each lane (figure 6-A). A densitometry analysis of the autoradiography is presented on the figure 6-B, in which a 2.5 fold increase of ERK-1 phosphorylation in response to a treatment with AZC can be visualized. Even if an increase in the kinase phosphorylation is usually relevant of kinase activation, we confirmed the increase in ERK-1 activity observed by performing kinase activity assays where the phosphorylation of Myelin Basic Protein (MBP) was analysed by SDS-PAGE and autoradiography. The densitometry analysis of the autoradiography of MBP is presented in figure 6-C. After a comparison with control, we can observe that MBP phosphorylation is increased 3 fold upon AZC treatment, which correlates the results obtained with kinase phosphorylation assays.

JNK-1 was the second kinase analysed for ER stress-induced activation. Using the same procedure as for ERK-1, the SDS-PAGE analysis of JNK-1 immunoprecipitated from the kinase phosphorylation assays was transferred onto a nitrocellulose membrane. The JNK-1 phosphorylation was assessed by autoradiography and we ensured that the same amount of JNK-1 protein was present in each of lane by performing an immunoblot with anti-JNK-1 antibodies (figure 7-A). The densitometry analysis of this autoradiography is presented on the figure 7-B; AZC and Tun treatments increased JNK-1 phosphorylation by 8.3 fold and 6.2 fold respectively. As for ERK-1 we confirmed the increase in JNK-1 activity by performing kinase activity assays in which the phosphorylation of the JNK-1 substrate GST-cJun was analysed. The densitometry analysis of the autoradiography of GST-cJun phosphorylation is presented in figure 6-C. The ER-induced JNK-1 activation caused an increase by 2.3 fold of GST-cJun phosphorylation upon AZC treatment, while an increase by 2 fold of JNK-1 substrate is visible upon Tun treatment.

The last kinase whose ER-mediated activation was reconstituted in our cell free assays was p38. We performed autoradiography on p38 immunoprecipitated from the kinase

phosphorylation assays; western blot analysis also confirmed that the same quantity of p38 proteins was present in each (figure 8-A). As it can be observed with the densitometry analysis of this autoradiography (figure 7-B), AZC and Tun treatments respectively increased p38 phosphorylation by 1.9 fold and 2.4 fold. As for ERK-1 we confirmed the increase in p38 activity by performing kinase activity assays in which the phosphorylation of the p38 substrate GST-ATF2 was analysed by SDS-PAGE and autoradiography. The densitometry analysis of this autoradiography is presented in figure 6-C. We can observe that the ER-mediated p38 activation in response to AZC and Tun treatment caused an increase in GST-ATF2 phosphorylation by 1.6 fold and 2.4 fold respectively.

Figure 5

Scheme of the cell-free kinase assays developed to study the ER-mediated activation of the MAPK/SAPKs

CNX-enriched compartment was immunopurified as described previously. To analyse the activation of a given kinase, the membrane sample was divided in two. As described in the Experimental procedure, one portion was used in the kinase phosphorylation assay and the other portion was kept to perform the kinase activation assay.

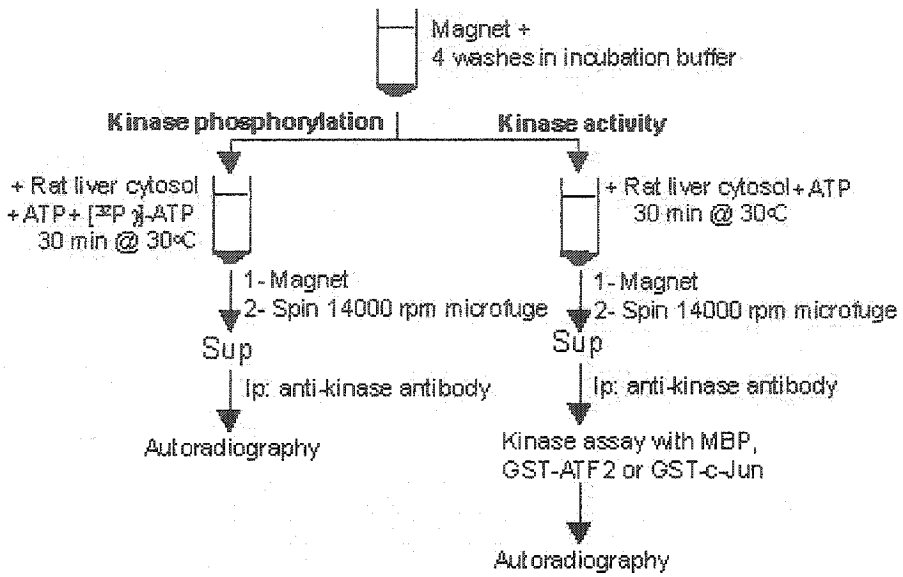
Magnet +
4 washes in incubation buffer
Kinase phosphorylation
Kinase activity
+ Rat liver cytosol
+ATP+ [³²P γ]-ATP
30 min @ 30°C
+ Rat liver cytosol+ATP
30 min @ 30°C
1- Magnet
2- Spin 14000 rpm microfuge
1- Magnet
2- Spin 14000 rpm microfuge
Sup
Sup
Ip: anti-kinase antibody
Ip: anti-kinase antibody
Autoradiography
Kinase assay with MBP,
GST-ATF2 or GST-c-Jun
Autoradiography

Figure 6

Activation of ERK-1 by isolated stressed ER

FR3T3 cells were treated with 10 mM azetidine-2 carboxylic acid (AZC), 2mM dithiothreitol (DTT), 10μg/ml tunicamycin (Tun) or 50 μM sodium arsenite (NaAs) and ER-like compartment was isolated as described in the Experimental procedures. 30 μg of immunopurified membranes were incubated with 3mg of rat liver cytosol for 30 min. at 30°C in a reaction buffer containing 0.1 mM ATP with or without 10μCi [^{32}Pγ]-ATP.

A) The upper panel shows the autoradiography of ERK-1 immunoprecipitated from the reaction performed with radiolabelled ATP (kinase phosphorylation assay); immunoblot of ERK-1 presented on the lower panel shows that the same amount of kinase is present in each lane.

B) Densitometry analysis of the autoradiography presented in A, ER isolated from AZC stressed cells increased ERK-1 phosphorylation by 2.5 fold. (n=3)

C) A kinase activity assay was performed with ERK-1 immunoprecipitated from the reaction where no [^{32}Pγ]-ATP was added; MBP was used as ERK-1 substrate and the kinase activity assay was analysed by SDS-PAGE and autoradiography. The graph represents the densitometry analysis of the autoradiography of MBP phosphorylation. The ER-induced ERK-1 activity is increased 3 fold with AZC treatment. (n=3)

A


Ctrl Azc DTT Tun NaAs
Ⓟ-ERK-1
Ib: αERK-1
Ip: αERK-1

B

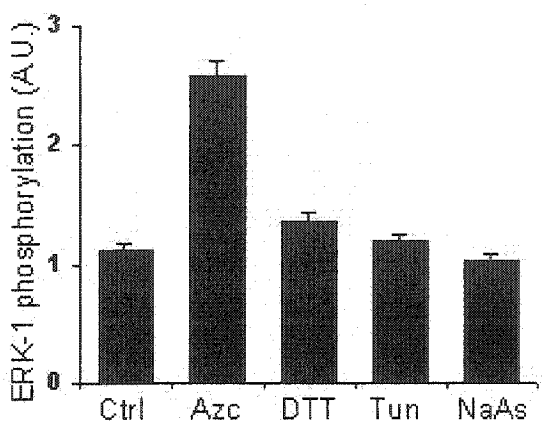
ERK-1 phosphorylation (A.U.)
0
1
2
3
Ctrl
Azc
DTT
Tun
NaAs

C

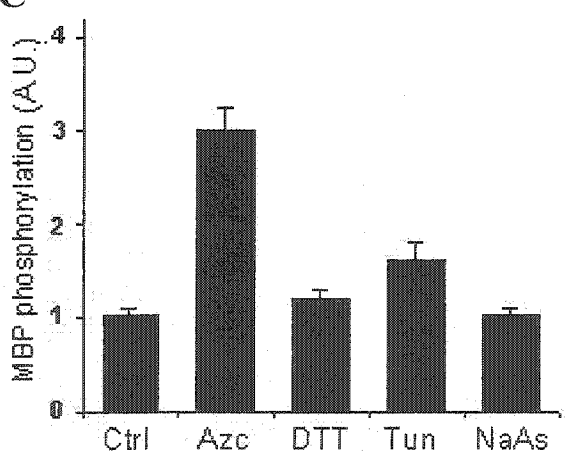
MBP phosphorylation (A.U.)
0
1
2
3
4
Ctrl
Azc
DTT
Tun
NaAs

Figure 7

Activation of JNK-1 by isolated stressed ER

FR3T3 cells were treated with 10 mM azetidine-2 carboxilic acid (AZC), 2mM dithiothreitol (DTT), 10μg/ml tunicamycin (Tun) or 50 μM sodium arsenite (NaAs) and ER-like compartment was isolated as described in the Experimental procedures. 30 μg of immunopurified membranes were incubated with 3mg of rat liver cytosol for 30 min. at 30°C in a reaction buffer containing 0.1 mM ATP with or without 10μCi [^{32}Pγ]-ATP.

A) The upper panel shows the autoradiography of JNK-1 immunoprecipitated from the reaction performed with radiolabelled ATP (kinase phosphorylation assay); immunoblot of JNK-1 presented on the lower panel shows that the same amount of kinase is present in each lane.

B) Densitometry analysis of the autoradiography presented in A; ER isolated from AZC and Tun stressed cells increased JNK-1 phosphorylation by 8.3 fold and 6.2 fold respectively.

C) A kinase activity assay was performed with JNK-1 immunoprecipitated from the reaction where no [^{32}Pγ]-ATP was added; GST-c-Jun was used as JNK-1 substrate and the kinase activity assay was analysed by SDS-PAGE and autoradiography. The graph represents the densitometry analysis of the autoradiography of GST-c-Jun phosphorylation. The ER-induced JNK-1 activity is increased 2.3 fold with AZC treatment and 2 fold with Tun treatment (n=3).

A

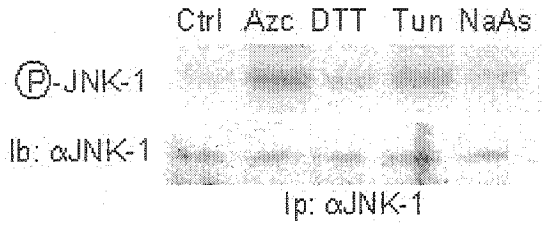
Ctrl Azc DTT Tun NaAs
Ⓟ-JNK-1
Ib: αJNK-1
Ip: αJNK-1

B

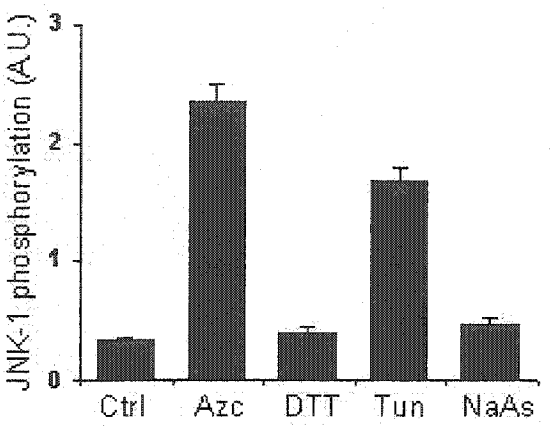
JNK-1 phosphorylation (A.U.)
3
2
1
0
Ctrl
Azc
DTT
Tun
NaAs

C

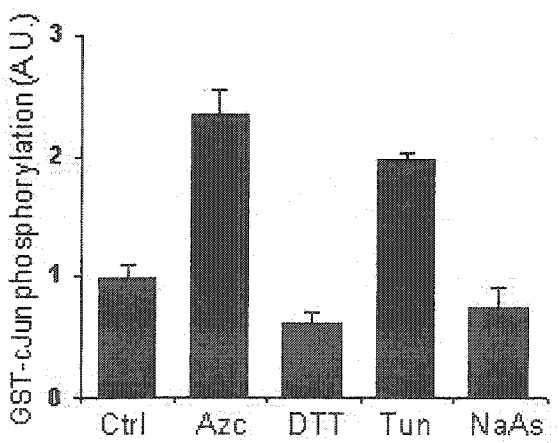
GST-cJun phosphorylation (A.U.)
3
2
1
0
Ctrl
Azc
DTT
Tun
NaAs

Figure 8

Activation of p38-1 by isolated stressed ER

FR3T3 cells were treated with 10 mM azetidine-2 carboxilic acid (AZC), 2mM dithiothreitol (DTT), 10μg/ml tunicamycin (Tun) or 50 μM sodium arsenite (NaAs) and ER-like compartment was isolated as described in the Experimental procedures. 30 μg of immunopurified membranes were incubated with 3mg of rat liver cytosol for 30 min. at 30°C in a reaction buffer containing 0.1 mM ATP with or without 10μCi [^{32}Pγ]-ATP.

A) The upper panel shows the autoradiography of p38 immunoprecipitated from the reaction performed with radiolabelled ATP (kinase phosphorylation assay); immunoblot of p38 presented on the lower panel shows that the same amount of kinase is present in each lane.

B) Densitometry analysis of the autoradiography presented in A; ER isolated from AZC and Tun stressed cells increased p38 phosphorylation by 1.9 fold and 2.4 fold respectively.

C) A kinase activity assay was performed with p38 immunoprecipitated from the reaction where no [^{32}Pγ]-ATP was added; GST-ATF2 was used as p38 substrate and the kinase activity assay was analysed by SDS-PAGE and autoradiography. The graph represents the densitometry analysis of the autoradiography of GST-ATF2 phosphorylation. The ER-induced p38 activity is increased 1.6 fold with AZC treatment and 2.4 fold with Tun treatment (n=3).

A

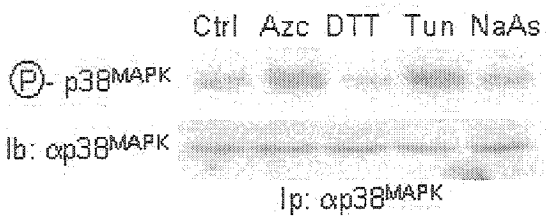
Ctrl Azc DTT Tun NaAs
Ⓟ- p38MAPK
Ib: αp38MAPK
Ip: αp38MAPK

B

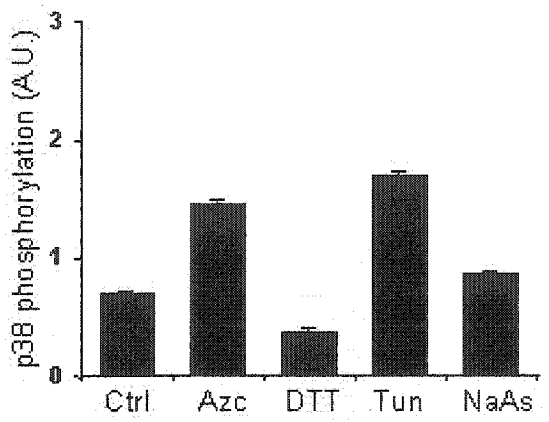
p38 phosphorylation (A.U.)
3
2
1
0
Ctrl
Azc
DTT
Tun
NaAs

C

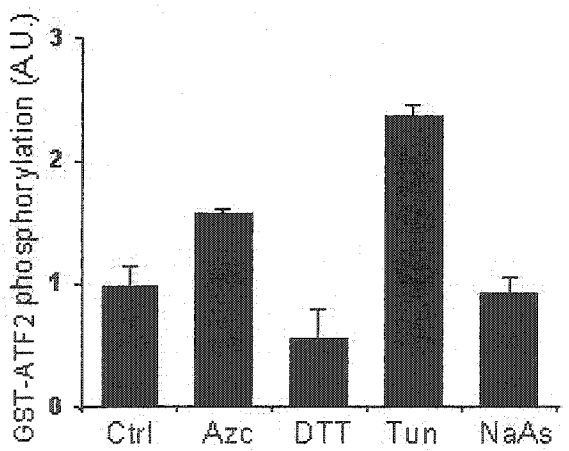
GST-ATF2 phosphorylation (A.U.)
3
2
1
0
Ctrl
Azc
DTT
Tun
NaAs

Involvement of Shc and Nck in the ER signalling

As exposed in the section Literature review, the activation of MAPK and SAPK commonly requires molecular adaptors such as Shc and Nck [100,102]; a pool of Shc adaptors and the small GTPase Ras were also localized at the ER membrane [106]. Consequently, we wanted to examine the possible contribution of these proteins to ER signalling. Since AZC was the only drug triggering an ER-mediated activation of all the kinases studied in this work, we decided to focus this analysis on AZC treatment.

We first ensured the presence of the two adaptors on the immuno-purified ER-like membranes isolated from cells treated or not with AZC. We performed western blot analysis for Shc and Nck as well as for CNX (figure 9), which is a control for the quantity of protein present in each lane because its expression is not influenced by ER stress. The presence of Shc and Nck can easily be visualized on both types of membranes. By comparing the panel representing the immunoblot for Shc to the one representing the immunoblot for CNX, we can observe that AZC treatment seems to decrease the amount of Shc at the ER-like compartment. A similar comparison for Nck immunoblot indicates that AZC as no significant effect on the amount of Nck associated with the ER-like membranes.

To assess the role of Shc and Nck adaptors in the ER-induced activation of the MAPK/SAPKs in response to AZC, we performed kinase phosphorylation assays and looked for perturbations of the reactions upon addition of GST constructs of Shc or Nck. To impair the functions of Shc, we added 10 µg of GST-Shc-SH2 to the kinase phosphorylation assays. Since Shc possess only two protein-interaction domains (SH2 and PTB) this construct disables the function of Shc [100]. For Nck, we added 5 µg of GST-Nck-$SH3_1$ and 5 µg of GST-Nck-$SH3_2$ to the reaction to prevent the interactions of Nck with the different kinases suggested to activate the SAPKs (NIK and PAK) and the binding of the adaptor SOS, which is required for ERK-1 activation [102]. An illustration of Shc and Nck molecules as well as the GST constructs used in the experiments is presented in figure 10-D. Finally, we also did control reactions to which were added 10

μg of GST alone. These three variants of the initial kinase phosphorylation assays were performed using ER-like compartments isolated from FR3T3 cells treated or not with 10 mM AZC.

The autoradiography of the SDS-PAGE analysis of ERK-1 immunoprecipitated from these reactions is presented at the figure 10-A (upper panel). The quantification of this autoradiography by densitometer analysis was used to calculate the ratio of phosphorylated ERK-1 (with AZC)/phosphorylated ERK-1 (no AZC) for each of the three variants of the kinase phosphorylation assays explained above; the values of the three ratio calculated are also illustrated on figure 10-A. By comparison to the ratio obtained for the reactions where only GST was added, we can observe that the increase in ERK-1 phosphorylation visible after AZC treatment is downregulated by 50% and 45% upon addition of GST constructs for Shc and Nck respectively.

The upper panel of the figure 10-B represents the autoradiography of the SDS-PAGE analysis of JNK-1 immunoprecipitated from the kinase phosphorylation assays explained above. We calculated the ratios of phosphorylated JNK-1 (with AZC)/phosphorylated JNK-1 (no AZC) from the quantification by densitometry of this autoradiography. The values of these ratios are exposed on the graph presented in figure 10-B. By comparing to the control value, the AZC-induced increase in JNK-1 phosphorylation was downregulated by 55% upon the addition of GST constructs for Nck while addition of GST-SH2-Shc increased the JNK-1 activity by 3.7 fold.

The results for the kinase phosphorylation assays performed for p38 are presented on figure 10-C. The upper panel represents the autoradiography of immunoprecipitated p38 and the values of the ratios calculated from the densitometry analysis are illustrated on the graph. A downregulation by 60% and 55% of the ER-mediated increase in p38 phosphorylation after AZC treatment can be visualized for the assays in which GST constructs for Shc and Nck were respectively added.

Altogether, the data presented above showed that Shc and Nck adaptors are present on the immuno-purified membranes and that their respective adaptor functions are involved in the modulation of MAPK/SAPKs during ER stress signalling. However, we wondered if the adaptors present on the ER-like compartments would be alone sufficient to account for the events observed at figure 10 or if the latter involved the adaptors present in the rat liver cytosol added to the reaction. To answer this question, we decided to perform the kinase phosphorylation assays using rat liver cytosols depleted in Shc or Nck. Again, these two variants of the kinase phosphorylation assays were done with ER-like compartments isolated from FR3T3 fibroblasts treated or not with AZC, since this drug is inducing an ER-mediated phosphorylation increase for all the kinases studied.

The depletion of Shc or Nck from the rat liver cytosol required two successive immunoprecipitations. The left side of figure 11-A corresponds to the western blot analysis of Shc immunodepletion experiment; lane 1, lane 2 and lane 3 represent respectively the crude rat liver cytosol, the cytosol after a first immunoprecipitation of Shc, and the cytosol depleted in Shc. The right side of figure 11-A corresponds to the same analysis done for Nck. The lane 4 represents Nck western blot on crud rat liver cytosol while the lane 6 corresponds to the cytosol devoid of Nck immunoreactivity.

We first performed kinase phosphorylation assays with the cytosol depleted in Shc. The kinases ERK-1, JNK-1 and p38 were immunoprecipitated from the reaction and analyzed by SDS-PAGE and transferred onto a nitrocellulose membrane, which was subjected to autoradiography (figure 11-B upper panel). The phosphorylation increases previously observed for all the kinases upon AZC treatment is downregulated when the Shc-immunodepleted cytosol is used in the reaction. To confirm that the same amount of kinase was immunoprecipitated from the assays, we performed an immunoblot with anti-ERK-1, anti-JNK-1 and anti-p38, which can be visualized at the bottom panel of figure 11-B; the same amount of the respective kinases is present in each lane. We also performed the kinase phosphorylation assays using the Nck-immunodepleted cytosol. The immunoprecipitations of ERK-1, JNK-1 and p38 from the reactions were analyzed by SDS-PAGE and transferred on nitrocellulose membrane. The figure 11-D represents the

autoradiography of that experiment where the increases in the phosphorylation of ERK-1 and JNK-1 normally visible after AZC treatment are downregulated following the use of the Nck-immunodepleted cytosol. The immunodepletion of Nck from the cytosol did not affect the phosphorylation status of p38, which was still increased upon drug treatment.

The results exposed in the previous paragraph confirmed the participation of Shc and Nck in the regulation of the MAPK/SAPKs. They also demonstrated that the amount of Shc and Nck adaptors present at the ER-like membranes was not sufficient to account for the activation of the MAPK/SAPKs observed upon drug treatments. This observation raised some concerns about the contribution of the ER signalling to the phenomenon observed since the property of the cytosol to amplify signals could generate artefacts. Indeed, a recent publication reported that a small fraction of the CNX pool is normally expressed on the surface of fibroblast cells [120].

Figure 9

Presence of Shc and Nck adaptors on the CNX-enriched membranes

ER-like compartments immunopurified from FR3T3 cells treated or not with 10mM AZC were analyzed by SDS-PAGE and immunoblotted for Shc (upper panel), Nck (mid panel) and CNX (lower panel). Shc and Nck adaptors are present on the ER-like compartment. AZC treatment reduces Shc presence at the ER-like membranes, but induces no changes for Nck; the anti-CNX immunoblot is used as a control for protein quantity.

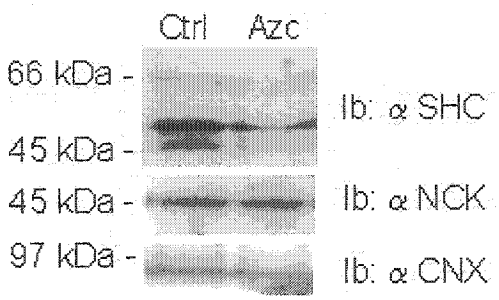
Ctrl
Azc
66 kDa -
45 kDa -
Ib: α SHC
45 kDa -
Ib: α NCK
97 kDa -
Ib: α CNX

Figure 10

Activation of MAPK/SAPKs by CNX-enriched membranes is modulated by Shc and Nck adaptors

ER-like compartments isolated from FR3T3 cells treated or not with 10 mM AZC were subjected to kinase phosphorylation assays to which were added either 10 μg of GST lane 1), 5 μg of GST-Nck-$SH3_1$ + 5 μg of GST-Nck-$SH3_2$ (lane 2) or 10 μg of GST-Shc-SH2 (lane 3). Immunoprecipitated ERK-1, JNK-1 or p38 were analyzed by SDS-PAGE and autoradiography (see Experimental procedures).

A) Phosphorylation levels of immunoprecipitated ERK-1 was assessed by autoradiography (upper panel) and quantified by densitometry analysis (graph). The quantification is expressed as the ratio of phosphorylated ERK-1 (+AZC)/ phosphorylated ERK-1 (-AZC). The AZC-induced ER-mediated increase in ERK-1 phosphorylation was downregulated by 50% and 45% upon the respective addition of GST constructs for Shc and Nck in the reactions.

B) The analysis described in (A) is pictured for the experiment concerning JNK-1. The AZC-induced ER-mediated increase in JNK-1 phosphorylation was downregulated by 55% upon the addition of GST constructs for Nck while addition of GST-SH2-Shc increased the JNK-1 activity by 3.7 fold.

C) The analysis described in (A) is pictured for the experiment concerning p38. The AZC-induced ER-mediated increase in p38 phosphorylation was downregulated by 60% and 55% upon the respective addition of GST constructs for Shc and Nck in the assays.

D) Representative scheme of the GST constructs for Shc (top) and Nck (bottom) used in the experiments.

A

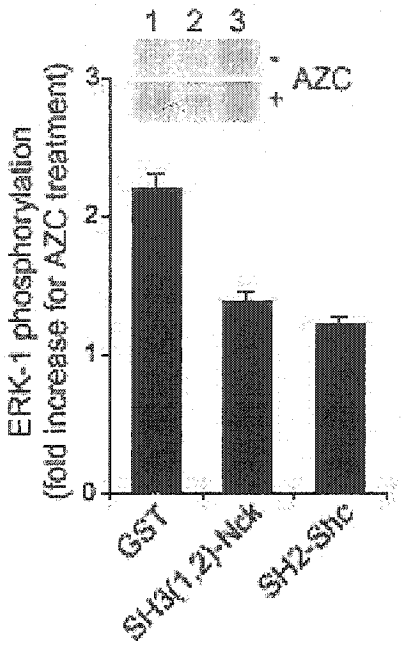
1 2 3
- AZC
+
ERK-1 phosphorylation
(fold increase for AZC treatment)
0
1
2
3
GST
SH3(1,2)-Nck
SH2-Shc

B

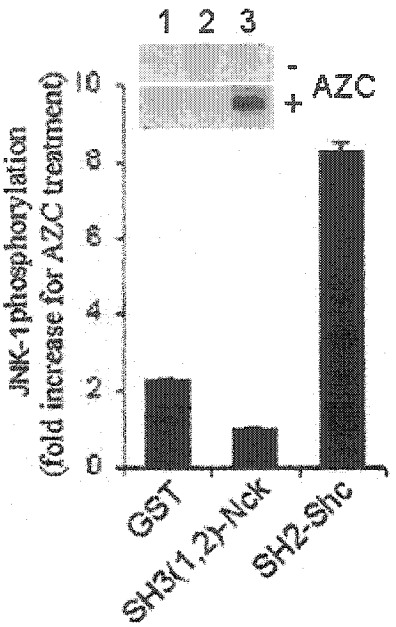
1 2 3
- AZC
+
JNK-1 phosphorylation
(fold increase for AZC treatment)
0
2
4
6
8
10
GST
SH3(1,2)-Nck
SH2-Shc

C

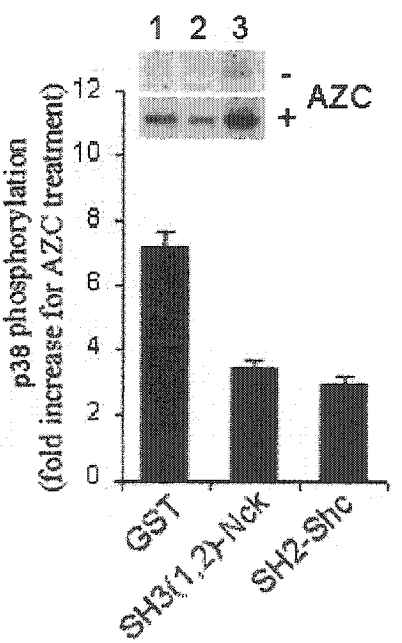
1 2 3
- AZC
+
p38 phosphorylation
(fold increase for AZC treatment)
0
2
4
6
8
10
12
GST
SH3(1,2)-Nck
SH2-Shc

D

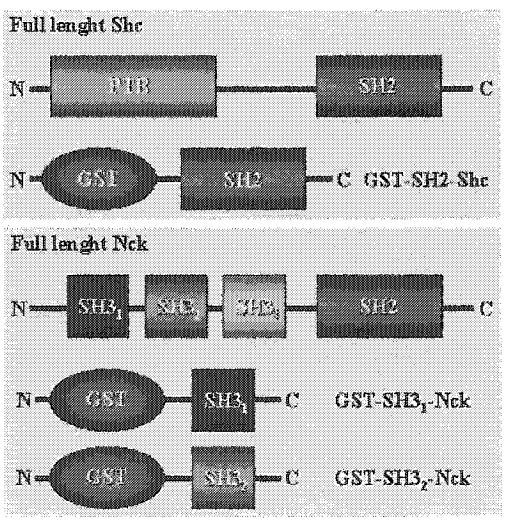
Full lenght Shc
N
PTB
SH2
C
N
GST
SH2
C
GST-SH2-Shc
Full lenght Nck
N
SH3
SH3
SH3
SH2
C
N
GST
SH3
C
GST-SH3-Nck
N
GST
SH3
C
GST-SH3-Nck

Figure 11

Shc and Nck immuno-depletion from cytosol impair the ER-induced activation of MAPK/SAPKs

A) Western blot analysis of the Shc and Nck immunodepletion from the cytosol; immunoblot with anti-Shc (on the left) and anti-Nck (on the right). Lanes 1, 2 and 4,5 represent respectively successive immunoprecipitations of Shc and Nck; lanes 3 and 6 show immunodepleted cytosols.

B) The upper panel shows the autoradiography of immunoprecipitations of ERK-1 (n=2), JNK-1 (n=3) and p38 (n=2) from kinase phosphorylation assays done with Shc-immunodepleted cytosols and analysed by SDS-PAGE. Kinases phosphorylation is downregulated when Shc is depleted from rat cytosol. The lower panel shows immunoblots with anti-ERK-1 (up), anti-JNK-1 (middle), and anti p38 (bottom) performed on the same SDS-PAGE analysis and it demonstrates that the amount of kinase is the same in each lane.

C) Autoradiography of immunoprecipitations of ERK-1 (n=2), JNK-1(n=3) and p38 (n=2) from kinase phosphorylation assays done with Nck-immunodepleted cytosols: kinases phosphorylation is downregulated except for p38.

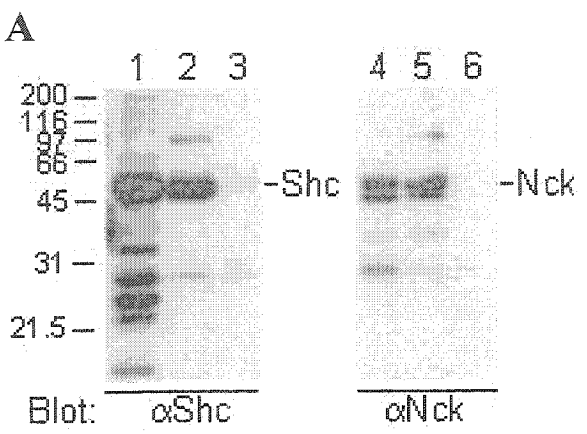
A
1 2 3
4 5 6
200
116
97
66
45
31
21.5
-Shc
-Nck
Blot:
αShc
αNck

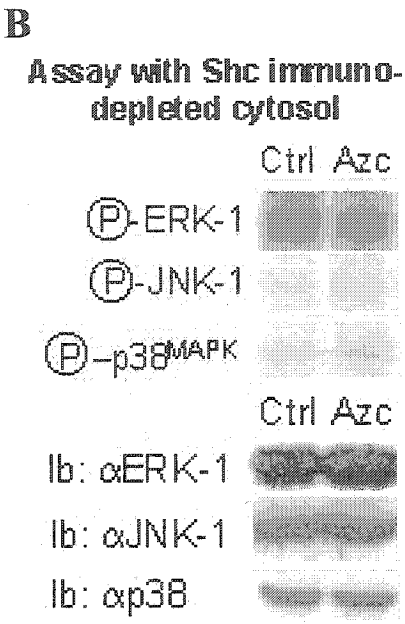
B
Assay with Shc immuno-depleted cytosol
Ctrl Azc
Ⓟ-ERK-1
Ⓟ-JNK-1
Ⓟ–p38MAPK
Ctrl Azc
Ib: αERK-1
Ib: αJNK-1
Ib: αp38

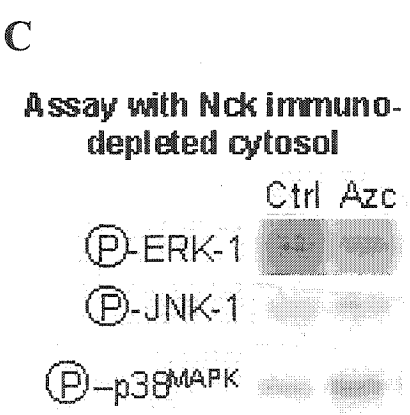
C
Assay with Nck immuno-depleted cytosol
Ctrl Azc
Ⓟ-ERK-1
Ⓟ-JNK-1
Ⓟ–p38MAPK

Plasma membrane signalling in response to ER stress inducers

We decided to assess the possible role of plasma membrane (PM) in the activation of MAPK/SAPKs in response to treatments with AZC, DTT, Tun and NaAs. We developed a protocol derived from the one used for the immuno-isolation of ER-like compartments to purify the PM. Since individual plasma membrane markers such as EGFR are usually expressed at low levels at the cell surface we could not use antibodies raised against a single molecule to isolate PM. We thus exploited the capacity of the lectin Wheat Germ Agglutinin (WGA) to interact with glycosylated proteins to affinity-purify a PM-like compartment given that most of the transmembrane proteins present at the PM are glycosylated at their extracellular portion [(1)]. By comparison to the procedure previously used for the immuno-isolation of CNX-enriched membranes, the only modification is the covalent fixation of WGA on the magnetic beads; a scheme of the affinity-purification of PM is illustrated at the figure 12-A.

We characterized the ER and the PM contents of the PM-like compartment by performing western blot analysis for EGFR (PM marker) and ribophorin I (ER marker) [(112)] on the crude cellular homogenate and the PM-like membranes. FR3T3 cells treated with AZC, DTT, Tun and NaAs were use in that characterization because we wanted to assess the possible effects of the different drug treatments on the content of the affinity-purify compartments. As illustrated on figure 12-B, the composition of the crude cellular homogenates and the PM-like membranes is not changing following the drug treatments. In addition, western blot analysis for EGFR (top panel) revealed enrichment by approximately 8 fold in PM content of the PM-like compartments compared to total homogenate. A similar comparison for the western blot of ribophorin I (bottom panel) allow us to conclude that the affinity-purified membranes are practically devoid of ER content.

We next incubated the PM-like compartments isolated from cells treated or not with AZC, DTT, Tun and NaAs with rat liver cytosol following the method described for kinase phosphorylation assays. Following the assays, the kinases ERK-1, JNK-1 and p38

were immunoprecipitated, separated by SDS-PAGE and transfer onto a nitrocellulose membrane. The first two panels of the figure 12-C represent the autoradiography of immunoprecipitated ERK-1 (first panel) and a subsequent immunoblot with anti-ERK-1 antibodies to ensure that the same amount of kinase was present in each lane (second panel). Together, these results support the fact that the phosphorylation status of ERK-1 is not modulated by PM no matter the drug treatment. The third and the fourth panel of the figure 12-C respectively illustrate the autoradiography and the control immunoblot for the assay concerning JNK-1. Again, none of the drugs administrated to the cells induced a PM-mediated activation of JNK-1. The autoradiography and the control immunoblot for the experiment in which p38 was immunoprecipitated are respectively depicted in the fifth and the sixth panel of the figure 12-C. Again, the same conclusion stands for p38 whose phosphorylation status is not regulated by the PM-like compartment regardless of the drug treatments. Altogether, these results excluded a possible contribution of the PM to the signalling events previously observed with the ER-like membranes, which confirmed that even if the rat liver cytosol amplifies the signal, the latter is specific to the CNX-enriched membranes.

Figure 12

Plasma membranes isolated from drug treated cells do not activate MAPK/SAPKs

A) Scheme of the experimental procedure used to affinity-purify plasma membrane-like membranes. The magnetic beads are coated with the lectin Wheat Germ Agglutinin, which binds to glycosylated transmembrane proteins expressed at the PM.

B) Biochemical characterization of the WGA-purified membranes. The upper panel represents an immunoblot for EGFR (PM marker) performed on WGA-purified membranes (top) and cellular homogenate (bottom) isolated from drug treated FR3T3 cells; plasma membranes en enriched approximately 8 fold in the WGA-bound fraction. The lower panel shows an immunoblot for Ribophorin 1 (ER marker) performed in the same conditions where a dramatic decrease in ER membranes can be visualized (n=2).

C) Kinase phosphorylation assay were done with WGA-purified PM isolated from FR3T3 cells treated or not with 10 mM azetidine-2 carboxylic acid (AZC), 2mM dithiothreitol (DTT), 10μg/ml tunicamycin (Tun) or 50 μM sodium arsenite (NaAs) and immunoprecipitated kinases were analysed by SDS-PAGE. The picture represents alternated autoradiography and immunoblot of ERK-1, JNK-1 and p38; WGA-purified PM does not activate kinases in response to the drugs tested.

A

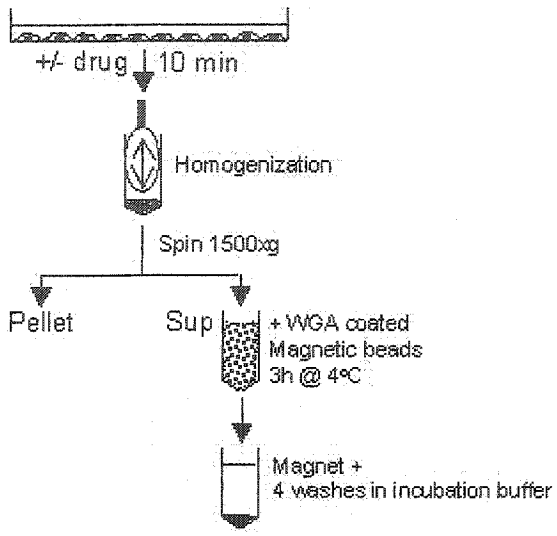
+/- drug
10 min
Homogenization
Spin 1500xg
Pellet
Sup
+ WGA coated
Magnetic beads
3h @ 4°C
Magnet +
4 washes in incubation buffer

B

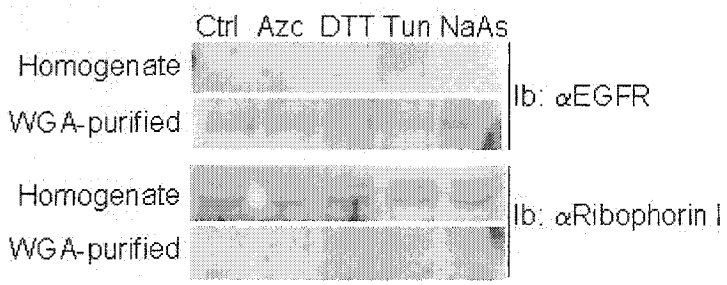
Ctrl Azc DTT Tun NaAs
Homogenate
WGA-purified
Ib: αEGFR
Homogenate
WGA-purified
Ib: αRibophorin I

C

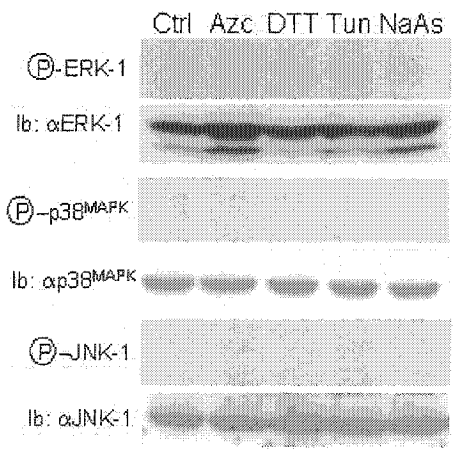
Ctrl Azc DTT Tun NaAs
Ⓟ-ERK-1
Ib: αERK-1
Ⓟ-p38MAPK
Ib: αp38MAPK
Ⓟ-JNK-1
Ib: αJNK-1

Activation of Shc and Nck in smooth and rough microsomes

When Shc and Nck are involved in a signalling cascade, they usually get phosphorylated and associated to the lipid bilayer. Moreover, the phosphorylation of these proteins induces conformational changes allowing their adaptor functions; it can also create binding site for other signalling molecules [100,102]. We thus wanted to analyse the phosphorylation status of Shc and Nck molecules present on the ER-like membranes isolated from cells subjected to ER stress-inducing drugs. Unfortunately, the immuno-purified compartment did not possess a strong enough intrinsic kinase activity to assess that question. We were also aware that the use of rat liver cytosol would probably give unreliable results since it could amplify the phosphorylation of the adaptors; the cytosol could also contain some kinases able to phosphorylate these adaptors regardless of the ER-mediated signalling.

In regard to the factors exposed above, we decided to assess the phosphorylation status of Shc and Nck associated with the ER membranes through the use of smooth microsomes (SM) and rough microsomes (RM) isolated from rat liver following a typical subcellular fractionation procedure [121]. RM and SM represent the fractions relative to rough ER and smooth ER membranes respectively [111]. The large amount of material obtained with a single procedure and the good intrinsic enzymatic activity of microsomes are among the positive aspects of this technique [122]. On the other hand, PM contamination commonly raises some concerns with regards to phosphorylation assays, but results presented earlier ruled out a possible contribution of PM to the signalling events triggered by ER stress.

We decided to study the ER-associated modulation of the Shc and Nck phosphorylation using RM and SM isolated from rat injected with Tun. We chose Tun because of its ability to travel easily through body tissues and cellular membranes and because of its capacity to induce cellular apoptosis [56]. Tun is known to induce the expression of markers for apoptosis in different tissues a few hours after the injection; for the kidney, apoptotic phenotypes can be visualized in tissues preparations a few days after the injection [56]. It should also be noted that Tun induces these effects when administrated at

sub-lethal doses such as 1μg/gram of body weight. Considering the properties of Tun, we decided to isolate the microsomes after an 18h treatment to make sure that the apoptotic signalling cascades susceptible to activate the adaptors are well activated; the protocol for the subcellular fractionation is described in details at the section Experimental procedures.

We first characterized the presence of Shc and Nck in RM and SM. The figure 13-A represents a western blot analysis for Shc, Nck and Bip performed on SM and RM isolated from animals injected or not with Tun. The immunoblot for Bip was performed to appreciate an increase in protein expression at the microsomes following Tun treatment; as mentioned in the section Literature review, Bip is an ER chaperone whose expression is upregulated following Tun-induced UPR. Bip expression in the two types of microsomes is increased following injection of Tun (figure 13-A, bottom panel). The upper panel figure 13-A pictures the western blot for Shc; a slight increase in Shc quantity can be observed in SM after Tun injection. We can also observe a very slight increase of Shc in RM following the drug treatment, but this variation is almost negligible. Unlike what was observed for Shc, the Nck quantity in the two types of microsomes undergoes a slight decrease upon Tun treatment (figure 13-A, mid panel).

To study the modulation of the phosphorylation status of Shc and Nck present on RM and SM following Tun treatment, we performed an in vitro phosphorylation assay in the presence of [^{32}Pγ]-ATP. Since RM and SM conserve a good intrinsic enzymatic activity, we just had to incubate the microsomes in a buffer solution adequate for enzymatic reactions (see Experimental procedures) [122]. After the assays, the microsomes were lysed and Shc or Nck adaptors were immunoprecipitated with their respective antibodies. Immunoprecipitated molecules were resolved by SDS-PAGE and subjected to autoradiography. The left panel of the figure 13-B represents the autoradiographies of Nck immunoprecipitated from RM and SM isolated from rat injected or not with Tun. An increase in Nck phosphorylation can be visualized following drug treatment in the two types of microsomes. The autoradiography of Shc is illustrated on the right panel of figure 13-B. A fair increase in Shc phosphorylation upon Tun-induced ER stress can be

visualized in SM. On the other hand, the phosphorylation of the adaptor is downregulated in RM isolated from drug treated animals.

The increase in the phosphorylation of Shc and Nck in SM in response to Tun could correlate with the activation of the adaptors present at the ER during the UPR. These results confirm a role of Shc and Nck in the ER stress signalling and support the idea that the ER-mediated activation of MAPK/SAPKs involves these adaptors.

Figure 13

Increased phosphorylation of Shc and Nck in smooth and rough rat liver microsomes in response to ER stress

Rat liver microsomes were isolated as described in Experimental procedures from rat injected or not with tunicamycin (1μg/gram of body weight).

A) SDS-PAGE analysis of smooth microsomes (SM) and rough microsomes (RM) immunoblotted with anti-Shc antibodies (upper panel), anti-Nck (middle panel) and anti-Bip (lower panel). By comparison with Bip, which is increased following Tun treatment in both SM and RM, a slight increase in Shc and a slight decrease in Nck can be observed in SM upon tunicamycin treatment, while the variations in the quantity of adaptors in RM are negligible (n=3).

B) An in vitro phosphorylation assay was performed with SM and RM isolated from tunicamycin-treated rats; Shc and Nck were immunoprecipitated an analysed by SDS-PAGE. The picture shows autoradiography of immunoprecipitated Nck (left panel) and Shc (right panel); the phosphorylation of both adaptors is increased in SM upon tunicamycin treatment.

A

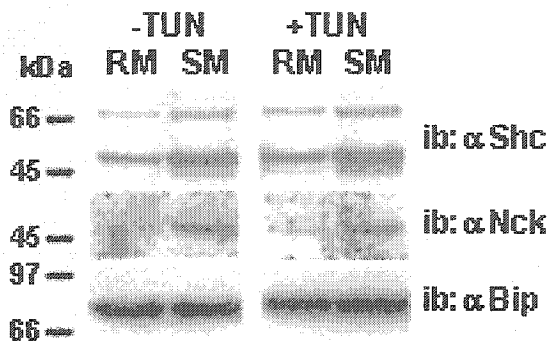
-TUN
+TUN
kDa
RM SM
RM SM
66
45
45
97
66
ib: α Shc
ib: α Nck
ib: α Bip

B

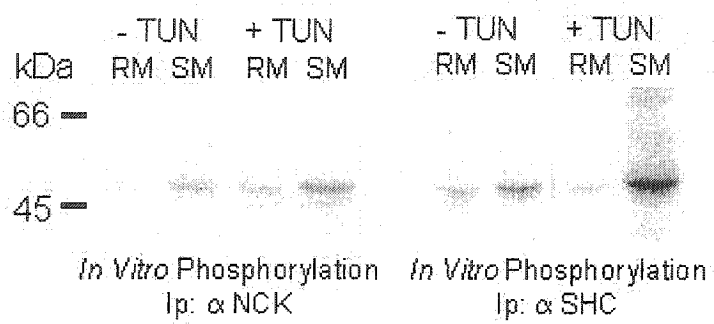
- TUN
+ TUN
- TUN
+ TUN
kDa
RM SM
RM SM
RM SM
RM SM
66
45
In Vitro Phosphorylation
Ip: α NCK
In Vitro Phosphorylation
Ip: α SHC

Discussion

The ability of magnetic beads to form covalent bounds with proteins is used in various fields of research [123]. Unlike many other protocol aimed at proteins or DNA isolation, we used this technique to isolate biological membranes. In fact, this work describes a new way to study the ER signalling based on the immunoisolation of an ER-like compartment using magnetic beads. Precedent work done in collaboration with our laboratory used anti-p23-coated magnetic beads to isolate Golgi vesicles in order to study the retrograde transport of Golgi enzymes [114]. We used anti-CNX-C4-coated magnetic beads in a similar fashion in order to study the ER signalling in response to stress (figure 2). Although the high level of expression and the wide distribution of CNX throughout the ER justified the use of CNX antibody to isolate a compartment similar to the whole ER (figure1), it would be interesting to immunopurify ER with antibodies raised against other transmembrane proteins. For instance, the Sec61 protein could be an adequate target to study the ER signalling occurring at the rough ER.

We assessed the quality and the morphology of ER-like compartments by electron microscopy (e.m.). The e.m. picture presented in figure 4 confirmed the ER resemblance of the ER-like membranes since it illustrates a large ER vesicle associated with some ribosomes. We also performed a biochemical analysis using antibodies for different organelle markers to further characterize the degree of purity of the immunoisolated membranes. The western blot analysis for CNX presented in figure 3 demonstrates enrichment in ER by approximately 15 fold of the ER-like compartments. Western blot analysis for EGFR and MG-160 indicated that the ER preparation presents a relatively high degree of purity since it is practically devoid of Golgi and PM (figure 3), which are classical contaminants of typical subcellular fractionation protocols. On the other hand, both e.m. and western blot analysis for Tom-20 revealed a mitochondrial contamination, which seems lower than in typical cellular fractionation procedures. This contamination can be explained by the tight junctions existing between the two organelles that play a role in the regulation of cellular Ca++ homeostasis [124,125]. Treatment of the cellular homogenate with chemicals such as EDTA [112] and KCl [87] used to strip the ribosomes

off the ER membranes might be useful to reduce mitochondrial contamination, but they may as well impair the binding of the antibodies to CNX. However, we were not worried by the presence of a little amount of mitochondria in our ER preparation since the only known mitochondrial signalling involves the release of Cytochrome C during cellular apoptosis [126].

Most of the early studies published on ER signalling used an approach centred on screens for yeast strains [21]. Following the cloning of the three mammalian ER stress-sensing signalling molecules, overexpression experiments were performed to characterize their mechanism of action in some details [23]. However, the effects of ER signalling on the kinases such as MAPKs and SAPKs involved in the cellular life or death decision remained obscure until very recently [72]. Here is presented for the first time an in vitro reconstitution of the ER-mediated regulation of ERK-1, JNK-1 and p38 in response to drug inducing protein misfolding. As presented in figure 5 we developed a cell free system in which the ER signalling was reconstituted by incubating the immunopurified ER-like compartments with rat liver cytosol. We demonstrated the ER-mediated activation of MAPK/SAPKs by performing kinase phosphorylation and kinase activity assays using this cell free system. Indeed, an increase in ERK-1 activity upon AZC treatment was clearly established in figure 6 where the densitometry analysis of kinase phosphorylation assays showed an increase by 2.5 fold of ERK-1 phosphorylation. The kinase activity assays performed following the same drug treatments also revealed an increased by 3 fold in ERK-1 activity upon AZC treatment (figure 6C). Surprisingly, DTT and Tun did not induce an ER-mediated activation of ERK-1; we expected an ERK-1 activation related to survival signals because the drug treatments were relatively short. We explain these results by the fact that both DTT and Tun are apoptosis inducers and that the specific signals sent by the ER might strictly be apoptotic. As expected, NaAs treatment did not trigger ERK-1 activation because this drug is not supposed to activate ER stress signalling. This is the first time the ER-induced ERK-1 activity is studied in response to drug inducing ER stress *in vitro*; it would be interesting to confirm these results *in vivo*. For instance, we could treat cells with a MEK1 inhibitor in addition to DTT or Tun to see if cells are more sensitive to ER-induced apoptosis. It would also be

of interest to study ERK-1 activation in response to other drugs causing ER-induced apoptosis such as brefeldin A and thapsigargin.

Unlike ERK-1, JNK-1 is activated in response to AZC and Tun (figure 7). The analysis of the kinase phosphorylation assay showed an increase in JNK-1 phosphorylation by 8.3 fold and 6.2 fold respectively. This increase in JNK-1 activity was confirmed with the analysis of the phosphorylation of GST-cJun, which was increased by 2.3 fold and 2 fold following AZC and Tun treatments. The JNK-1 activation upon AZC and Tun treatments was expected since these drugs induce ER-stress and that the drug Tun is able to induce cellular apoptosis. It is interesting to mention that a recent publication demonstrated an implication of Rac1 and JNK in the upregulation of heath shock factors in response to AZC [127]. We were intrigued to see no activation of JNK-1 in response to DTT since pro-apoptotic effects are attributed to this drug. Indeed, Ron's group demonstrated that Ire1 activates JNK-1 through TRAF2 in response to DTT and Tun, but their kinase assays were performed using the lysates of DTT-stressed rat pancreatic acinar AR42J cells [72]. It should be notice that a DTT-induced ER-mediated activation of JNK-1 might not observed in fibroblast cell lines; such activation may also required fully developed apoptotic phenotype which needs a longer drug exposure. As for the ERK-1 assays, NaAs treatment did not trigger ERK-1 activation, which concords with the fact that this drug is not supposed to activate ER stress signalling [119].

Finally, we also tested the kinase p38 for an ER-mediated regulation in response to ER stress inducers. The results exposed in figure 8 demonstrated an increase in the p38 phosphorylation by 1.9 fold and 2.4 fold following AZC and Tun treatments. The upregulation of p38 activity in response to these drugs was also observed through phosphorylation of GST-ATF2, which was increased by 1.6 fold with AZC and 2.4 fold with Tun. Similarly to JNK-1, we expected the ER-mediated activation of p38 following treatments with AZC and Tun since these kinases are involved in stress and apoptosis signalling. These findings corroborate the data published by another group, which demonstrated that CHOP requires a p38-mediated phosphorylation to be fully activated during Tun-induced apoptosis [128]. By comparing the results obtained for Tun and AZC

treatments, we suggest that AZC is not able to induce apoptosis like Tun because it triggers the activation of ERK-1. Indeed, ERK-1 has anti-apoptotic functions and its activation during ER stress might be sufficient to allow cell survival. It would be interesting to treat fibroblast cells with AZC and a MEK1 inhibitor to add additional evidences supporting that hypothesis.

Surprisingly, the analysis of the results for both kinase phosphorylation assays and kinase activity assays did not show any activation of p38 upon DTT treatment. We suggest that either p38 is not involved in the signalling cascades related to DTT treatment, but we could also think that p38 activation requires an advanced state of apoptosis, which would need a longer drug treatment. Again, we did not observe a p38 activation following NaAs treatment, which was expected since this drug is not supposed to activate ER stress signalling. This control also allow us to conclude that signalling molecules such as p38 cannot associate with the ER-like membrane in a non-specific manner because NaAs-induced cellular stress was shown to activate p38 in NIH3T3 cells [129]. From the data presented above, we conclude that we successfully reconstituted the ER signalling in a cell free system and that we provided *in vitro* evidences for the ER-mediated activation of MAPK/SAPKs.

Given that Shc and Nck molecules are commonly involved in the activation of MAPKs and SAPKs, we hypothesized that these molecular adaptors would modulate the activation ERK-1, JNK-1 and p38 observed in response to AZC treatment. The results presented in figure 9 confirmed the presence of Shc and Nck adaptors on the ER-like membranes immunoisolated from fibroblast treated or not with AZC. It is interesting to mention that AZC slightly decreased the amount of Shc at the ER-like compartment, which opposes the recruitment of the adaptor to the lipid bilayer associated with its activation. This phenomenon might be related to the proteolytic cleavage of transmembrane signalling proteins that occurs during UPR [42,45]. Nevertheless, we assumed that GST constructs for the protein/protein interaction domains of Shc and Nck would perturb in the kinase phosphorylation assays related to AZC. This theory was well funded since the Shc construct inhibited the AZC-induced ER-mediated activation of

ERK-1 by 50% and p38 by 60%. Surprisingly, GST-SH2-Shc increased the JNK-1 activity by 3.7 fold. We hypothesize that the construct binds to and activates a kinase upstream of JNK-1 in a manner that could be specific or not; the construct might also inhibit a phosphatase responsible for JNK-1 downregulation. The addition of Nck constructs to the kinase phosphorylation assays caused no surprises because it has downregulated the ER-mediated activation of all the kinases. The activation of ERK-1 was inhibited by 45% and the activity of JNK-1 and p38 were downregulated by 55%. Altogether, these data confirmed the role of Shc and Nck adaptors in the ER signalling and, more specifically, in the ER-mediated activation of the MAPK/SAPK in response to AZC. It would be of interest to push further the analysis of these signalling cascades through the addition of specific kinase inhibitors in the assays.

To provide additional evidences supporting the implication of the adaptors in the ER signalling, we performed kinase phosphorylation assays using ER-like compartments and rat liver cytosols depleted in Shc or Nck. The depletion of the adaptors from the cytosols would also indicate if the adaptors present at the ER-like compartments were sufficient for the activation of ERK-1, JNK-1 and p38 in response to AZC. The depletion of Shc or Nck from the rat cytosols required two successive immunoprecipitations as illustrated by the western blot analysis presented in figure 10-A. As expected, the upregulation of ERK-1, JNK-1 and p38 usually observed upon AZC treatment was practically abolished in the kinase phosphorylation assays performed with Shc-depleted cytosols (figure 10-B). These results together with the observation that GST-Shc-SH2 impaired the AZC-induced upregulation of ERK-1 and JNK-1 support the involvement of Shc in the ER signalling. We can also conclude that the Shc proteins present in the rat liver cytosol are absolutely required for the transmission of signals from the ER to the cytosolic kinases.

Similarly to what was observed for Shc, the use of Nck-depleted cytosols strongly downregulated AZC-induced activation of ERK-1 and JNK-1 (figure 10-C). However, the amount of Nck adaptors present at the ER-like membranes seemed to be sufficient to maintain the increase in the phosphorylation of p38 triggered by AZC treatment. Alternatively, these results could also mean that Nck is not involved in the ER-mediated

regulation of p38. If this is the case, the perturbation of the AZC-induced p38 activation observed with the Nck GST constructs might be related to non-specific interactions of the constructs with SH3-binding signalling molecules upstream of p38. Many different experimental approaches including the use of fibroblast cells isolated from mice deficient in Nck could be used to clarify the involvement of Nck in ER-mediated p38 activation.

The fact that the adaptors present in the cytosol account for most of the Shc and Nck proteins required for the ER signalling occurring in our cell free system raised some concerns about the specificity of the ER signal amplified. Indeed, a recent publication reported that a small fraction of CNX pool is normally expressed on the surface of fibroblast cells [120]. A very small contamination of the ER-like membrane preparation with PM could thus be amplified by the rat liver cytosol. To assess the possible contribution of the PM to the ER signalling reconstituted in the cell free system, we purified PM-like compartments using magnetic beads coated with WGA (figure 12-A). The western blot analysis for EGFR revealed enrichment in PM by approximately 8 fold of the PM-like membranes compared to crude homogenate (figure 12-B). A similar comparison for the western blot analysis concerning the ER marker showed that the PM-like compartments were practically devoid of ER contamination. This partial biochemical analysis also confirmed that none of the drug treatments altered the composition of the PM-like compartments.

The kinase phosphorylation assays performed with the affinity purified PM demonstrated that PM is not involved in the signalling response observed following treatment with ER stress-inducing drugs. Indeed, a PM-mediated increase in the phosphorylation of ERK-1 was not observed with PM-like compartments isolated from cells treated or not with AZC, DTT, Tun, or NaAs; the same observation can be made with assays concerning JNK-1 and p38 (figure 12-C). As mentioned earlier, a recent publication demonstrated the activation of p38 in response to NaAs-induced cellular stress [129]; we suggest that PM is not involved in that phenomenon. Further more, we hypothesize that that PM signalling is not activated in early cellular reaction to AZC, DTT and Tun. It might be interesting to analyse the PM signalling and the cellular

susceptibility to these ER stress-inducing drugs in fibroblast grown at a confluence of 100%. Although the procedure used to purify PM-like membranes concerned a control experiment, this new approach to study PM signalling could be useful for many other research projects regarding PM signalling or PM proteomic characterization.

Finally, we investigated the modulation of the phosphorylation of the Shc and Nck adaptors localized at the ER membranes. Since the activation of these molecules is associated with their phosphorylation and their relocalization to the lipid bilayer, we hypothesized that treatment with ER stress inducers would increase the phosphorylation of Shc and Nck. We decided to use another approach to test that hypothesis because the immuno-purified compartment did not possess a strong enough intrinsic kinase activity. In addition, the use of rat liver cytosol could give unreliable results by amplifying the phosphorylation of the adaptors. Even if a small PM contamination can occur during the isolation of the rat livers microsomes [111] we used this system to study the effect of Tun on the phosphorylation of the adaptors. In fact, the results obtained with affinity-purified PM-like compartments suggested that PM is not involved in the response to treatments with ER stress-inducing drugs. It should be specified that microsomes possess a good intrinsic enzymatic activity and that a procedure using a few rat liver gives a large amount of material [122].

We first characterize the presence of the adaptors Shc and Nck at SM and RM isolated from rat treated or not with Tun (figure 13-A). As control for upregulation of protein expression during Tun-induced stress, we also performed western blot for Bip. A slight increase in Shc quantity in SM can be observed upon Tun treatment; the increase in Shc at RM membranes is almost negligible. This upregulation of Shc expression at microsomal membranes is consistent with the activation of the adaptor and its implication in a signalling cascade. Unlike Shc, Nck quantity in both types of microsomes seems to undergo a slight decrease following Tun treatment. This phenomenon might be explained by the involvement of a pool of Nck in a cytoskeletal reorganization that could accompany the enlargement of the ER *in vivo* [130]. Alternatively, this event might be related to the proteolytic processing of ER resident stress signalling molecules [42,45].

We performed in vitro phosphorylation assays with SM and RM to study the modulation of the phosphorylation of Shc and Nck following ER stress induction (figure 13-B). A fair increase in Shc phosphorylation upon Tun-induced ER stress can be observed in SM. This result correlates the upregulation of Shc presence at SM membranes observed above since both events can be related to the activation of the molecule. Conversely, Tun injection seems to downregulate the phosphorylation of Shc in RM. We hypothesize that Shc might be relocated from rough to smooth ER membrane for *in vivo* signalling. Unlike what is reported for Shc, Nck phosphorylation is increased in SM and RM following Tun treatment. This observation suggests that the Nck adaptors present on the microsomes after Tun treatment are fairly activated since we noticed a slight decrease in Nck expression in SM and RM following the same conditions. These results could be consistent with the hypothesis that a pool of Nck is relocated to the cytoskeleton during ER stress, but further evidences are needed to support the existence of such phenomenon. It would be interesting to use fibroblast isolated from of Nck knockout mice to assess the ER morphology during UPR. Altogether, the results illustrated in figure 13 provide additional evidences for the implication Shc and Nck in the ER signalling in response to stress. Given that SM seems to contain more Shc and Nck adaptors, and that both molecules are activated in SM in response to Tun, we also suggest that smooth ER is more active than rough ER during the signalling triggered by the accumulation of misfolded proteins.

In conclusion, we report here a new method to study ER signalling based on the immunoisolation of an ER-like compartment with anti-CNX-coated magnetic beads. We demonstrate that this compartment can be used in a cell free system to reproduce the ER signalling in response to stress. We show that this compartment contains per se the information required for the activation of MAPK and SAPKs. Indeed, we demonstrate that the CNX-enriched compartment is mediating the activation of ERK-1, JNK-1 and p38 upon AZC treatment and that Tun induces an ER-mediated activation of JNK-1 and p38. In addition, we report a new method to isolate the PM using WGA-coated magnetic beads and we demonstrate that the affinity purified PM-like compartments do not activate

MAPK/SAPKs during AZC, DTT, Tun and NaAs treatments. Furthermore, we provide evidences for the involvement of Shc and Nck in the ER signalling and we observe that these adaptors modulate the ER-mediated activation of MAPK/SAPKs.

We hypothesize that ER-mediated activation of the MAPK ERK-1 could occur through Shc and/or Nck adaptors and the small GTPase Ras since the recent finding that small GTPases of the Ras superfamily are targeted to the ER through their CAAX motif [107,108]. In addition, we suggest that the ER-mediated activation of the SAPKs occurring through Shc involves Ras and the subsequent activation of Rac or Cdc42, given that these small GTPases have been associated with the activation of JNK-1 and p38 [98-100]. We theorize that the involvement of Nck in the activation of the SAPKs require the activation of the kinase PAK and/or NIK. While PAK in known to activate SAPKs trough the small GTPases Rac and Cdc42, NIK was demonstrated to activate MEKK1, which is a MAPKKK leading to the upregulation of JNK activity [102-104]. Finally, we put forward the idea that the ER signalling could use the classical signalling mechanisms occurring at the PM, which involve the dimerization and the transactivation of transmembrane receptor followed by the recruitment of adaptor/docking molecules. However, an association of Shc and Nck adaptors with ER-resident signalling proteins such as IRE1 and PERK as not yet been demonstrated. Since RTKs are synthesized and deactivated at the ER [105], we can also hypothesize that ER-resident chaperone could mediate their activation during UPR. Clearly, the mechanisms of activation and the functions of the MAPK/SAPKs concerning the ER signalling are intriguing and would require further investigations. It would be interesting to study the implication of other kinases of the ERK and JNK families in the ER stress and to further characterize the p38 isoforms involved in the ER signalling.

This work extends the repertoire of signalling molecules associated with ER stress signalling as well as the number of cytosolic kinases whose activities are modulated during the ER stress response. This study together with other works recently published are beginning to unravel the complex interactions between the ER and the cytosol, which will hopefully give a better perspective on the mechanisms operating during the

determination of the cellular fate in response to ER stress-inducing drugs. A better understanding of the ER stress response is critical for advances in the fight against important diseases such as Alzheimer disease and spongiform encephalopathies, which are related to a chronic ER stress signalling [17].

References

1) Voet D. and Voet J.G. (1995). Biochemistry. Second edition. John Wiley and Sons Inc.

2) Alberts B. and coll. (1989). Biologie moléculaire de la cellule (translation). Second edition. Flammarion

3) MacKrill, J. J. (1999). Protein-protein interactions in intracellular Ca2+-release channel function. Biochem J **337**(Pt 3): 345-61.

4) Corbett, E. F., K. Oikawa, et al. (1999). Ca2+ regulation of interactions between endoplasmic reticulum chaperones. J Biol Chem **274**(10): 6203-11.

5) Meldolesi J. and T. Pozzan (1998). The endoplasmic reticulum Ca2+ store: a view from the lumen. Trends Biochem Sci **23**(1): 10-4

6) Pahl, H. L. (1999). Signal transduction from the endoplasmic reticulum to the cell nucleus. Physiol Rev **79**(3): 683-701.

7) Johnson, A. E. (1997). Protein translocation at the ER membrane: a complex process becomes more so. Trends Cell Biol **7**:90-4

8) Johnson, A. E. and M. A. van Waes (1999). The translocon: a dynamic gateway at the ER membrane. Annu Rev Cell Dev Biol **15**: 799-842.

9) Laitusis, A. L., M. A. Brostrom, et al. (1999). The dynamic role of GRP78/BiP in the coordination of mRNA translation with protein processing. J Biol Chem **274**(1): 486-93.

10) Miller, J. D., S. Tajima, et al. (1995). The beta subunit of the signal recognition particle receptor is a transmembrane GTPase that anchors the alpha subunit, a peripheral membrane GTPase, to the endoplasmic reticulum membrane. J Cell Biol **128**(3): 273-82

11) Fedorov, A. N. and T. O. Baldwin (1997). Cotranslational protein folding. J Biol Chem **272**(52): 32715-8.

12) Ellgaard, L., M. Molinari, et al. (1999). Setting the standards: quality control in the secretory pathway. Science **286**(5446): 1882-8.

13) Mori, K. (2000). Tripartite management of unfolded proteins in the endoplasmic reticulum. Cell **101**(5): 451-4.

14) Helenius, A. and M. Aebi (2001). Intracellular functions of N-linked glycans. Science **291**(5512): 2364-9.

15) Sousa, M. and A. J. Parodi (1995). The molecular basis for the recognition of misfolded glycoproteins by the UDP-Glc:glycoprotein glucosyltransferase. Embo J **14**(17): 4196-203.

16) Kopito, R. R. (1997). ER quality control: the cytoplasmic connection. Cell **88**(4): 427-30.

17) Aridor, M. and W. E. Balch (1999). Integration of endoplasmic reticulum signaling in health and disease. Nat Med **5**(7): 745-51.

18) Kaufman, R. J. (1999). Stress signaling from the lumen of the endoplasmic reticulum: coordination of gene transcriptional and translational controls. Genes Dev **13**(10): 1211-33.

19) Sidrauski, C., R. Chapman, et al. (1998). The unfolded protein response: an intracellular signalling pathway with many surprising features. Trends Cell Biol **8**(6): 245-9.

20) Patil, C. and P. Walter (2001). Intracellular signaling from the endoplasmic reticulum to the nucleus: the unfolded protein response in yeast and mammals. Curr Opin Cell Biol **13**(3): 349-55.

21) Chapman, R., C. Sidrauski, et al. (1998). Intracellular signaling from the endoplasmic reticulum to the nucleus. Annu Rev Cell Dev Biol **14**: 459-85.

22) Welihinda, A. A., W. Tirasophon, et al. (1997). Gene induction in response to unfolded protein in the endoplasmic reticulum is mediated through Ire1p kinase interaction with a transcriptional coactivator complex containing Ada5p. Proc Natl Acad Sci U S A **94**(9): 4289-94.

23) Ma, Y. and L. M. Hendershot (2001). The unfolding tale of the unfolded protein response. Cell **107**(7): 827-30.

24) Urano, F., A. Bertolotti, et al. (2000). IRE1 and efferent signaling from the endoplasmic reticulum. J Cell Sci **113 Pt 21**: 3697-702

25) Welihinda, A. A., W. Tirasophon, et al. (2000). The transcriptional co-activator ADA5 is required for HAC1 mRNA processing in vivo. J Biol Chem **275**(5): 3377-81.

26) Shamu, C. E. and P. Walter (1996). Oligomerization and phosphorylation of the Ire1p kinase during intracellular signaling from the endoplasmic reticulum to the nucleus. Embo J **15**(12): 3028-39.

27) Okamura, K., Y. Kimata, et al. (2000). Dissociation of Kar2p/BiP from an ER sensory molecule, Ire1p, triggers the unfolded protein response in yeast. Biochem Biophys Res Commun **279**(2): 445-50.

28) Sidrauski C., J. S. Cox et al. (1996). tRNA ligase is required for regulated mRNA splicing in the unfolded protein response. Cell **87**: 405-13

29) Welihinda, A. A., W. Tirasophon, et al. (1998). Protein serine/threonine phosphatase Ptc2p negatively regulates the unfolded-protein response by dephosphorylating Ire1p kinase. Mol Cell Biol **18**(4): 1967-77.

30) Tirasophon, W., A. A. Welihinda, et al. (1998). A stress response pathway from the endoplasmic reticulum to the nucleus requires a novel bifunctional protein kinase/endoribonuclease (Ire1p) in mammalian cells. Genes Dev **12**(12): 1812-24.

31) Wang, X. Z., H. P. Harding, et al. (1998). Cloning of mammalian Ire1 reveals diversity in the ER stress responses. Embo J **17**(19): 5708-17.

32) Liu, C. Y., M. Schroder, et al. (2000). Ligand-independent dimerization activates the stress response kinases IRE1 and PERK in the lumen of the endoplasmic reticulum. J Biol Chem **275**(32): 24881-5.

33) Bertolotti, A., Y. Zhang, et al. (2000). Dynamic interaction of BiP and ER stress transducers in the unfolded-protein response. Nat Cell Biol **2**(6): 326-32.

34) Yoshida, H., T. Matsui, et al. (2001). XBP1 mRNA is induced by ATF6 and spliced by IRE1 in response to ER stress to produce a highly active transcription factor. Cell **107**(7): 881-91.

35) Liou, H.C., M.R. Boothby, et al. (1990) A new member of the leucine zipper class of proteins that binds to the HLA DRα promoter. Science **247**(4950): 1581-4

36) Yoshida, H., K. Haze, et al. (1998). Identification of the cis-acting endoplasmic reticulum stress response element responsible for transcriptional induction of mammalian glucose-regulated proteins. Involvement of basic leucine zipper transcription factors. J Biol Chem **273**(50): 33741-9.

37) Tirasophon, W., K. Lee, et al. (2000). The endoribonuclease activity of mammalian IRE1 autoregulates its mRNA and is required for the unfolded protein response. Genes Dev **14**(21): 2725-36.

38) Iwawaki, T., A. Hosoda, et al. (2001). Translational control by the ER transmembrane kinase/ribonuclease IRE1 under ER stress. Nat Cell Biol **3**(2): 158-64.

39) Zhu, C., F. E. Johansen, et al. (1997). Interaction of ATF6 and serum response factor. Mol Cell Biol **17**(9): 4957-66.

40) Parker, R., T. Phan, et al. (2001). Identification of TFII-I as the endoplasmic reticulum stress response element binding factor ERSF: its autoregulation by stress and interaction with ATF6. Mol Cell Biol **21**(9): 3220-33.

41) Wang, Y., J. Shen, et al. (2000). Activation of ATF6 and an ATF6 DNA binding site by the endoplasmic reticulum stress response. J Biol Chem **275**(35): 27013-20.

42) Chen, X., J. Shen, et al. (2002). The luminal domain of ATF6 senses endoplasmic reticulum (ER) stress and causes translocation of ATF6 from the ER to the Golgi. J Biol Chem **277**(15): 13045-52.

43) Ye, J., R.B. Rawson, et al (2000). ER stress induces cleavage of membrane-bound ATF6 by the same proteases that process SREBPs. Mol Cell **6**:1355-64

44) Haze, K., T. Okada, et al. (2001). Identification of the G13 (cAMP-response-element-binding protein-related protein) gene product related to activating transcription factor 6 as a transcriptional activator of the mammalian unfolded protein response. Biochem J **355**(Pt 1): 19-28

45) Niwa, M., C. Sidrauski, et al. (1999). A role for presenilin-1 in nuclear accumulation of Ire1 fragments and induction of the mammalian unfolded protein response. Cell **99**(7): 691-702.

46) Katayama, T., K. Imaizumi, et al. (1999). Presenilin-1 mutations downregulate the signalling pathway of the unfolded-protein response. Nat Cell Biol **1**(8): 479-85.

47) Sato, N., F. Urano, et al. (2000). Upregulation of BiP and CHOP by the unfolded-protein response is independent of presenilin expression. Nat Cell Biol **2**(12): 863-70.

48) Harding, H. P., Y. Zhang, et al. (1999). Protein translation and folding are coupled by an endoplasmic-reticulum-resident kinase. Nature **397**(6716): 271-4

49) Harding, H. P., Y. Zhang, et al. (2000). Perk is essential for translational regulation and cell survival during the unfolded protein response. Mol Cell **5**(5): 897-904.

50) Williams, B. R. (1999). PKR; a sentinel kinase for cellular stress. Oncogene **18**(45): 6112-20.

51) Harding, H. P., H. Zeng, et al. (2001). Diabetes mellitus and exocrine pancreatic dysfunction in perk-/- mice reveals a role for translational control in secretory cell survival. Mol Cell **7**(6): 1153-63.

52) Scheuner, D., B. Song, et al. (2001). Translational control is required for the unfolded protein response and in vivo glucose homeostasis. Mol Cell 7(6): 1165-76.

53) Brewer, J. W. and J. A. Diehl (2000). PERK mediates cell-cycle exit during the mammalian unfolded protein response. Proc Natl Acad Sci U S A 97(23): 12625-30

54) Harding, H. P., I. Novoa, et al. (2000). Regulated translation initiation controls stress-induced gene expression in mammalian cells. Mol Cell 6(5): 1099-108.

55) Okada, T., H. Yoshida, et al. (2002). Distinct Roles of ATF6 and PERK in Transcription during the Mammalian Unfolded Protein Response. Biochem J **16** pub ahead

56) Zinszner, H., M. Kuroda, et al. (1998). CHOP is implicated in programmed cell death in response to impaired function of the endoplasmic reticulum. Genes Dev **12**(7): 982-95

57) Novoa, I., H. Zeng, et al. (2001). Feedback inhibition of the unfolded protein response by GADD34-mediated dephosphorylation of eIF2alpha. J Cell Biol **153**(5): 1011-22.

58) Romisch, K. (1999). Surfing the Sec61 channel: bidirectional protein translocation across the ER membrane. J Cell Sci **112**(Pt 23): 4185-91.

59) Parodi, A. J. (2000). Role of N-oligosaccharide endoplasmic reticulum processing reactions in glycoprotein folding and degradation. Biochem J **348 Pt 1**: 1-13.

60) Spear, E. and D. T. Ng (2001). The unfolded protein response: no longer just a special teams player. Traffic **2**(8): 515-23.

61) Friedlander, R., E. Jarosch, et al. (2000). A regulatory link between ER-associated protein degradation and the unfolded-protein response. Nat Cell Biol **2**(7): 379-84.

62) Travers, K. J., C. K. Patil, et al. (2000). Functional and genomic analyses reveal an essential coordination between the unfolded protein response and ER-associated degradation. Cell **101**(3): 249-58.

63) Bonifacino, J. S. and A. M. Weissman (1998). Ubiquitin and the control of protein fate in the secretory and endocytic pathways. Annu Rev Cell Dev Biol **14**: 19-57.

64) Bays, N. W., R. G. Gardner, et al. (2001). Hrd1p/Der3p is a membrane-anchored ubiquitin ligase required for ER-associated degradation. Nat Cell Biol **3**(1): 24-9.

65) Ferri, K. F. and G. Kroemer (2001). Organelle-specific initiation of cell death pathways. Nat Cell Biol **3**(11): E255-63.

66) McCullough, K. D., J. L. Martindale, et al. (2001). Gadd153 sensitizes cells to endoplasmic reticulum stress by down- regulating Bcl2 and perturbing the cellular redox state. Mol Cell Biol **21**(4): 1249-59.

67) Wang, X. Z. and D. Ron (1996). Stress-induced phosphorylation and activation of the transcription factor CHOP (GADD153) by p38 MAP Kinase. Science **272**(5266): 1347-9.

68) Nakagawa, T., H. Zhu, et al. (2000). Caspase-12 mediates endoplasmic-reticulum-specific apoptosis and cytotoxicity by amyloid-beta. Nature **403**(6765): 98-103

69) Mehmet, H. (2000). Caspases find a new place to hide. Nature **403**(6765): 29-30.

70) Yoneda, T., K. Imaizumi, et al. (2001). Activation of caspase-12, an endoplastic reticulum (ER) resident caspase, through tumor necrosis factor receptor-associated factor 2-dependent mechanism in response to the ER stress. J Biol Chem **276**(17): 13935-40.

71) Nakagawa, T. and J. Yuan (2000). Cross-talk between two cysteine protease families. Activation of caspase-12 by calpain in apoptosis. J Cell Biol **150**(4): 887-94.

72) Urano, F., X. Wang, et al. (2000). Coupling of stress in the ER to activation of JNK protein kinases by transmembrane protein kinase IRE1. Science **287**(5453): 664-6.

73) Ng, F. W., M. Nguyen, et al. (1997). p28 Bap31, a Bcl-2/Bcl-XL- and procaspase-8-associated protein in the endoplasmic reticulum. J Cell Biol **139**(2): 327-38.

74) Ng, F. W. and G. C. Shore (1998). Bcl-XL cooperatively associates with the Bap31 complex in the endoplasmic reticulum, dependent on procaspase-8 and Ced-4 adaptor. J Biol Chem **273**(6): 3140-3.

75) Cohen, G. M. (1997). Caspases: the executioners of apoptosis. Biochem J **326**:1-16.

76) Maatta, J., O. Hallikas, et al. (2000). Limited caspase cleavage of human BAP31. FEBS Lett **484**(3): 202-6.

77) Nguyen, M., D. G. Breckenridge, et al. (2000). Caspase-resistant BAP31 inhibits fas-mediated apoptotic membrane fragmentation and release of cytochrome c from mitochondria. Mol Cell Biol **20**(18): 6731-40.

78) Zuppini, A., J. Groenendyk, et al. (2002). Calnexin deficiency and endoplasmic reticulum stress-induced apoptosis. Biochemistry **41**(8): 2850-8.

79) Pahl, H. L. and P. A. Baeuerle (1995). A novel signal transduction pathway from the endoplasmic reticulum to the nucleus is mediated by transcription factor NF-kappa B. Embo J **14**(11): 2580-8.

80) Thevenin, C., S.-J. Kim, et al. (1991). Induction of nuclear factor-κB and the human immunodeficiency virus long terminal repeat by okadaic acid, a specific inhibitor of phosphatases 1and 2A. Nature New Biol **2**:793-800.

81) Pahl, H. L. and P. A. Baeuerle (1997). The ER-overload response: activation of NF-kappa B. Trends Biochem Sci **22**(2): 63-7.

82) Nozaki, S., G. W. Sledge Jr, et al. (2001). Repression of GADD153/CHOP by NF-kappaB: a possible cellular defense against endoplasmic reticulum stress-induced cell death. Oncogene **20**(17): 2178-85.

83) Pahl, H. L. and P. A. Baeuerle (1996). Activation of NK-κB by ER stress requires both Ca++ and reactive oxygen intermediates as messengers. FEBS Lett. 392: 129-36

84) Pahl, H. L., M. Sester, et al. (1996). Activation of NK-κB by adenovirus E3/19K requires its ER-retention. J.Cell Biol **132**: 511-22.

85) Roderick, H. L., J. D. Lechleiter, et al. (2000). Cytosolic phosphorylation of calnexin controls intracellular Ca(2+) oscillations via an interaction with SERCA2b. J Cell Biol **149**(6): 1235-48.

86) Schue, V., G. A. Green, et al. (1994). Hyperphosphorylation of calnexin, a chaperone protein, induced by Clostridium difficile cytotoxin. Biochem Biophys Res Commun **203**(1): 22-8.

87) Chevet, E., H. N. Wong, et al. (1999). Phosphorylation by CK2 and MAPK enhances calnexin association with ribosomes. Embo J **18**(13): 3655-66.

88) Nakamura, K., E. Bossy-Wetzel, et al. (2000). Changes in endoplasmic reticulum luminal environment affect cell sensitivity to apoptosis. J Cell Biol **150**(4): 731-40.

89) Caspersen, C., P. S. Pedersen, et al. (2000). The sarco/endoplasmic reticulum calcium-ATPase 2b is an endoplasmic reticulum stress-inducible protein. J Biol Chem **275**(29): 22363-72.

90) Thuerauf, D.J., H. Hoover, et al. (2001). Sarco/endoplasmic Reticulum Calcium ATPase-2 Expression Is Regulated by ATF6 during the Endoplasmic Reticulum Stress Response. J Biol Chem **276** (51): 48309-17

91) Leonardi, A., P. Vito, et al. (2002). Endoplasmic Reticulum Stress Causes Thyroglobulin Retention in this Organelle and Triggers Activation of Nuclear Factor-kappaB Via Tumor Necrosis Factor Receptor-Associated Factor 2. Endocrinology **143**(6): 2169-77.

92) Tibbles, L. A. and J. R. Woodgett (1999). The stress-activated protein kinase pathways. Cell Mol Life Sci **55**(10): 1230-54.

93) Ichijo, H. (1999). From receptors to stress-activated MAP kinases. Oncogene **18**(45): 6087-93

94) Hagemann, C. and J. L. Blank (2001). The ups and downs of MEK kinase interactions. Cell Signal **13**(12): 863-75.

95) Bradley, J. R. and J. S. Pober (2001). Tumor necrosis factor receptor-associated factors (TRAFs). Oncogene **20**(44): 6482-91

96) Coso O. A., M. Chiariello, et al. (1995) The small GTP-binding proteins Rac1 and Cdc42 regulate the activity of the JNK/SAPK signaling pathway. Cell **81**(7): 1137–1146.

97) Jaffer, Z. M. and J. Chernoff (2002). p21-Activated kinases: three more join the Pak. Int J Biochem Cell Biol **34**(7): 713-7.

98) Minden, A., A. Lin, et al. (1995). Selective activation of the JNK signaling cascade and c-Jun transcriptional activity by the small GTPases Rac and Cdc42Hs. Cell **81**(7): 1147-57.

99) Hashimoto, A., M. Kurosaki, et al. (1999). Shc regulates epidermal growth factor-induced activation of the JNK signaling pathway. J Biol Chem **274**(29): 20139-43.

100) Ravichandran, K. S. (2001). Signaling via Shc family adapter proteins. Oncogene **20**(44): 6322-30.

101) Melamed, I., H. Patel, et al. (1999). Activation of Vav and Ras through the nerve growth factor and B cell receptors by different kinases. Cell Immunol **191**(2): 83-9.

102) McCarty, J. H. (1998). The Nck SH2/SH3 adaptor protein: a regulator of multiple intracellular signal transduction events. Bioessays **20**(11): 913-21.

103) Chong, C., L. Tan, et al. (2001). The mechanism of PAK activation: Autophosphorylation events in both regulatory and kinase domains control activity. J Biol Chem **276**(20): 17347-53.

104) Su, Y. C., J. Han, et al. (1997). NIK is a new Ste20-related kinase that binds NCK and MEKK1 and activates the SAPK/JNK cascade via a conserved regulatory domain. Embo J **16**(6): 1279-90.

105) Haj, F. G., P. J. Verveer, et al. (2002). Imaging sites of receptor dephosphorylation by PTP1B on the surface of the endoplasmic reticulum. Science **295**(5560): 1708-11.

106) Lotti, L. V., L. Lanfrancone, et al. (1996). Sch proteins are localized on endoplasmic reticulum membranes and are redistributed after tyrosine kinase receptor activation. Mol Cell Biol **16**(5): 1946-54.

107) Choy, E., V. K. Chiu, et al. (1999). Endomembrane trafficking of ras: the CAAX motif targets proteins to the ER and Golgi. Cell **98**(1): 69-80.

108) Michaelson, D., J. Silletti, et al. (2001). Differential localization of Rho GTPases in live cells: regulation by hypervariable regions and RhoGDI binding. J Cell Biol **152**(1): 111-26.

109) Romano, J. D., W. K. Schmidt, et al. (1998). The Saccharomyces cerevisiae prenylcysteine carboxyl methyltransferase Ste14p is in the endoplasmic reticulum membrane. Mol Biol Cell **9**(8): 2231-47.

110) Schmidt, W. K., A. Tam, et al. (1998). Endoplasmic reticulum membrane localization of Rce1p and Ste24p, yeast proteases involved in carboxyl-terminal CAAX protein processing and amino-terminal a-factor cleavage. Proc Natl Acad Sci U S A **95**(19): 11175-80.

111) Dallner, G. (1974). Isolation of rough and smooth microsomes--general. Methods Enzymol **31**(Pt): 191-201.

112) Walter, P. and G. Blobel (1983). Preparation of microsomal membranes for cotranslational protein translocation. Methods Enzymol **96**: 84-93.

113) Luers, G. H., R. Hartig, et al. (1998). Immuno-isolation of highly purified peroxisomes using magnetic beads and continuous immunomagnetic sorting. Electrophoresis **19**(7): 1205-10.

114) Lin, C. C., H. D. Love, et al. (1999). ER/Golgi intermediates acquire Golgi enzymes by brefeldin A-sensitive retrograde transport in vitro. J Cell Biol **147**(7): 1457-72.

115) Wada, I., D. Rindress, et al. (1991). SSR alpha and associated calnexin are major calcium binding proteins of the endoplasmic reticulum membrane. J Biol Chem **266**(29): 19599-610.

116) Ou, W. J., J. J. Bergeron, et al. (1995). Conformational changes induced in the endoplasmic reticulum luminal domain of calnexin by Mg-ATP and Ca2+. J Biol Chem **270**(30): 18051-9.

117) Chevet, E., G. Lemaitre, et al. (1999). Identification and characterization of an intracellular protein complex that binds fibroblast growth factor-2 in bovine brain. Biochem J **341**(Pt 3): 713-23. **MG-160**

118) Schleiff, E., G. C. Shore, et al. (1997). Interactions of the human mitochondrial protein import receptor, hTom20, with precursor proteins in vitro reveal pleiotropic specificities and different receptor domain requirements. J Biol Chem **272**(28): 17784-9 **TOM-20**

119) Brostrom, C. O., C. R. Prostko, et al. (1996). Inhibition of translational initiation by activators of the glucose-regulated stress protein and heat shock protein stress response systems. Role of the interferon-inducible double-stranded RNA-activated eukaryotic initiation factor 2alpha kinase. J Biol Chem **271**(40): 24995-5002.

120) Okazaki, Y., H. Ohno, et al. (2000). Cell surface expression of calnexin, a molecular chaperone in the endoplasmic reticulum. J Biol Chem **275**(46): 35751-8.

121) Paiement, J. and J. J. Bergeron (1983). Localization of GTP-stimulated core glycosylation to fused microsomes. J Cell Biol **96**(6): 1791-6.

122) Ou, W. J., D. Y. Thomas, et al. (1992). Casein kinase II phosphorylation of signal sequence receptor alpha and the associated membrane chaperone calnexin. J Biol Chem **267**(33): 23789-96.

123) Web site of Dynal Biotech, www.dynalbiotech.com

124) Rizzuto, R., P. Pinton, et al. (1998). Close contacts with the endoplasmic reticulum as determinants of mitochondrial Ca2+ responses. Science **280**(5370): 1763-6.

125) Wang, H. J., G. Guay, et al. (2000). Calcium regulates the association between mitochondria and a smooth subdomain of the endoplasmic reticulum. J Cell Biol **150**(6): 1489-98.

126) Duchen, M. R. (2000). Mitochondria and calcium: from cell signalling to cell death. J Physiol **529 Pt 1**: 57-68.

127) Han, S. I., S. Y. Oh, et al. (2001). Implication of a small GTPase Rac1 in the activation of c-Jun N-terminal kinase and heat shock factor in response to heat shock. J Biol Chem **276**(3): 1889-95.

128) Maytin, E. V., M. Ubeda, et al. (2001). Stress-inducible transcription factor CHOP/gadd153 induces apoptosis in mammalian cells via p38 kinase-dependent and -independent mechanisms. Exp Cell Res **267**(2): 193-204.

129) Kim, J. Y., J. A. Choi, et al. (2002). Involvement of p38 mitogen-activated protein kinase in the cell growth inhibition by sodium arsenite. J Cell Physiol **190**(1): 29-37.

130) Li, W., J. Fan, et al. (2001). Nck/Dock: an adapter between cell surface receptors and the actin cytoskeleton. Oncogene **20**(44): 6403-17.